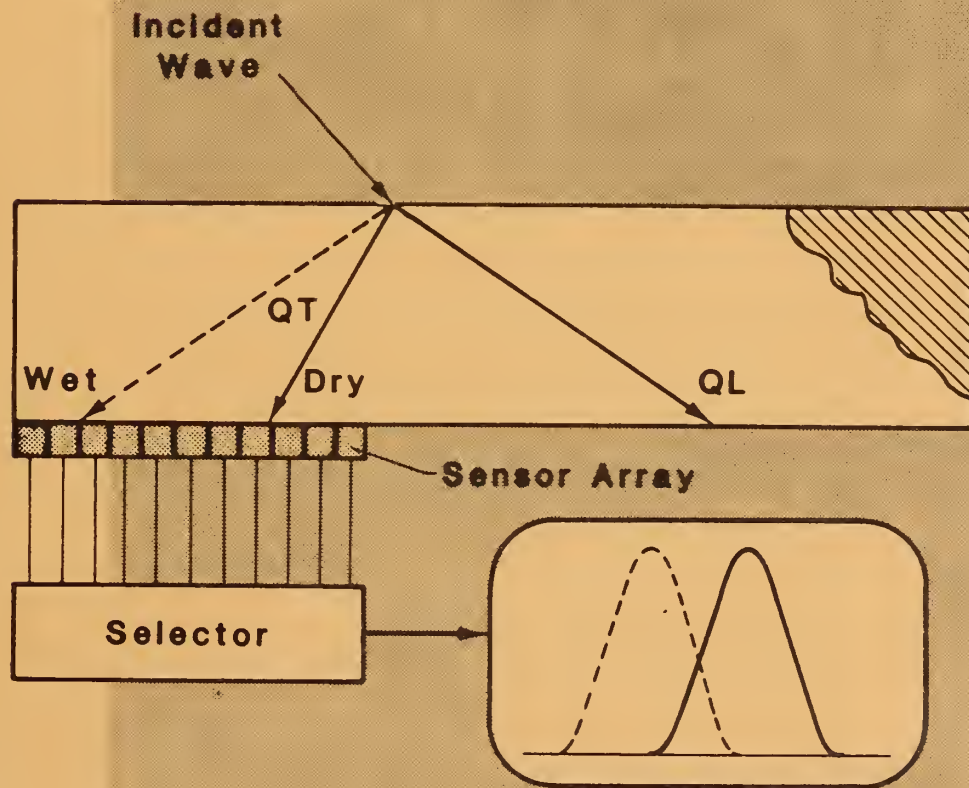


Institute for Materials Science and Engineering

# FRACTURE AND DEFORMATION

NAS-NRC  
Assessment Panel  
February 2-3, 1989



NISTIR 88-3841  
U.S. Department of Commerce  
National Institute of Standards  
and Technology

QC  
100  
.U56  
88-3841  
1988  
C.2

## Technical Activities 1988

For a unidirectional graphite-fiber-reinforced epoxy-matrix composite, the direction of stress wave propagation is influenced by small changes in elastic properties caused by saturation (WET) of the epoxy matrix from a dehydrated (DRY) state. Only the quasitransverse (QT) wave is affected by small changes in elastic properties. The unaffected quasilongitudinal (QL) wave propagates along a preferred path of fiber orientation, which is shown in the cutaway view. The array of transducers along with appropriate circuitry (selector) is used to display an insitu shift in the received stress wave.

Reported by: 1. R.D. Kriz, "Monitoring Elastic Stiffness Degradation in Graphite/Epoxy Composites," in *Solid Mechanics Research for Quantitative Non-Destructive Evaluation*, Dordrecht, The Netherlands: Martinus Nijhoff, 1987, pp. 389–395. 2. Patent No. 4,499,770, Feb. 19, 1985. 3. D.W. Fitting, R.D. Kriz, and A.V. Clark, "Measuring In-plane Elastic Moduli of Composites with Arrays of Phase-Insensitive Ultrasound Receivers," in *Review of Progress in Quantitative NDE*, New York: Plenum in press.

ISTC QC 100 .U56 no. 88-3841 1989

**IMSE**

Institute for Materials Science and Engineering

# **FRACTURE AND DEFORMATION**

---

H.I. McHenry, Chief

NAS-NRC  
Assessment Panel  
February 2-3, 1989

NISTIR 88-3841  
U.S. Department of Commerce  
National Institute of Standards and Technology  
October 1988

## **Technical Activities 1988**

Research Information Center  
National Institute of Standards  
and Technology  
Gaithersburg, Maryland 20899



CONTENTS

DIVISION ORGANIZATION . . . . . iv

INTRODUCTION . . . . . 1

RESEARCH STAFF . . . . . 5

TECHNICAL ACTIVITIES . . . . . 9

    Performance . . . . . 11

        Fracture Mechanics . . . . . 11

        Fracture Physics . . . . . 17

        Nondestructive Evaluation. . . . . 21

        Composites . . . . . 31

    Properties . . . . . 39

        Cryogenic Materials. . . . . 39

        Physical Properties. . . . . 48

    Processing. . . . . 55

        Welding. . . . . 55

        Thermomechanical Processing. . . . . 59

OUTPUTS AND INTERACTIONS . . . . . 65

    Selected Recent Publications . . . . . 67

    Selected Technical and Professional Committee Leadership. . . . . 74

    Awards. . . . . 76

    Industrial and Academic Interactions . . . . . 77

APPENDIX . . . . . 83

    Fracture and Deformation Division . . . . . 85

    Institute for Materials Science and Engineering . . . . . 86

    National Institute of Standards and Technology. . . . . 87

## DIVISION ORGANIZATION

Harry I. McHenry, Chief  
(303) 497-3268

### PERFORMANCE

Fracture Mechanics	David T. Read (303) 497-3853
Fracture Physics	Ing-Hour Lin (303) 497-5791
Nondestructive Evaluation	Alfred V. Clark, Jr. (303) 497-3159
Composites	Ronald D. Kriz (303) 497-3547

### PROPERTIES

Cryogenic Materials	Richard P. Reed (303) 497-3870
Physical Properties	Hassel M. Ledbetter (303) 497-3443

### PROCESSING

Welding	Thomas A. Siewert (303) 497-3523
Thermomechanical Processing	Yi-Wen Cheng (303) 497-5545

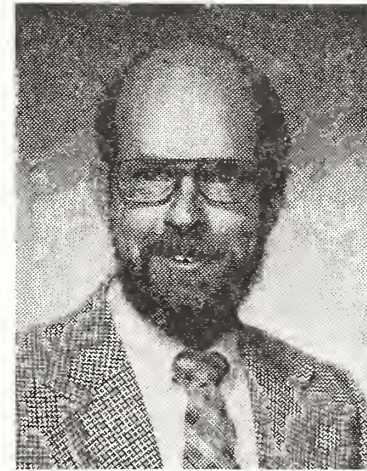
### ADMINISTRATIVE SUPPORT

Administrative Officer	Kathy S. Sherlock (303) 497-3288
Division Secretary	Heidi M. Quartemont (303) 497-3251
Group Secretaries	Vonnie J. Edgins (303) 497-5338 Chris J. King (303) 497-5350

# INTRODUCTION



## FRACTURE AND DEFORMATION DIVISION



Harry I. McHenry  
Chief

The research of the Fracture and Deformation Division is directed toward improving the structural safety and fostering the use of advanced materials. Research on fracture mechanics, nondestructive evaluation, and welding technology contributes to the safe and efficient performance of materials in structural applications. The development of better deformation-processing methods and quality-control sensors improves the processing and properties of advanced materials. Deformation and fracture studies based on solid-state physics and dislocation mechanics provide a basic understanding of the structure and physical properties of advanced materials and the role of imperfections.

Our interdisciplinary staff is organized into specific research groups in the general areas of materials performance, properties, and processing. Each group is headed by a recognized expert in that technology who provides a focal point for industrial cooperations, scientific interactions, and technology transfer.

Historically, the division has emphasized materials research to improve structural safety, but now we are directing more of our efforts toward the National Institute of Standards and Technology goal of increased industrial competitiveness. In support of the long-range plan of the Institute of Materials Science and Engineering, our new programs focus on advanced materials with high commercial potential and emphasize research on materials processing, which is the key to improved productivity in the metals industry. We also conduct materials research for other government agencies and provide technical services to industries, universities, and other scientific laboratories.

Improving structural safety and fostering the use of advanced materials is essential to increase the competitiveness of American industry. Fracture and its prevention cost the U.S. economy 4 percent of our GNP (\$116 billion in 1981, the year of the NBS-Battelle study for Congress); industry can save about 50 percent of these costs by technological means. The market for advanced materials is projected to reach \$80 billion by the year 2000, and the value of new products made from these materials is substantially greater.

American industry leads the world in the development of advanced materials, but frequently we trail in using these materials for commercial products. The commercial lag is due to lack of confidence in the service performance of advanced materials, particularly safety and reliability. The Fracture and Deformation Division programs are developing measurement methods, sensors, standards, and reference data that will be used to measure the quality of advanced materials and to assess their service performance. Once measurement methods and standards are developed, industry can confidently use advanced materials to design and manufacture new products.

# RESEARCH STAFF



- Austin, Mark W.
- Elastic properties
  - X-ray diffraction
- Berger, J. R.
- Fracture mechanics
  - Photo mechanics
  - Dynamic fracture
- Cheng, Yi-Wen
- Fatigue of metals
  - Fracture behavior of surface flaws
  - Fatigue-life predictions
  - Thermomechanical processing of steels
- Clark, Alfred V., Jr.
- Theoretical and experimental ultrasonics
  - Engineering mechanics
  - Nondestructive evaluation
- Delgado, Luz M.
- Mechanical testing
  - Compilation of low-temperature reference data
- Fitting, Dale W.
- Sensor arrays for NDE
  - Ultrasonic and radiographic NDE
  - Signal and image processing
  - NDE of composites
- Heyliger, Paul R.
- Computational mechanics
  - Finite-element methods
  - Mechanics of composite materials
- Kim, Sudook
- Elastic properties
  - Low-temperature physical properties
  - Ultrasonics
- Kriz, Ronald D.
- Finite-element analysis for composites
  - Mechanics of composite materials
  - NDE of composite materials
- Ledbetter, Hassel M.
- Physical properties of solids
  - Theory and measurement of elastic constants
  - Physical properties of austenitic steels
  - Measurement and modeling of physical properties of composite materials
  - Martensite-transformation theory
- Lin, Ing-Hour
- Fracture-toughening mechanisms
  - Ductile-brittle transition
  - Elastic interactions of cracks and defects
  - Dynamic deformation and fracture
  - Dislocation theory

- McCowan, Chris N.
- Welding metallurgy
  - Mechanical properties at low temperatures
  - Metallography and fractography
- McHenry, Harry I.
- Fracture mechanics
  - Low-temperature materials
  - Fracture control
- Purtscher, Pat T.
- Fracture properties of high-strength steels
  - Metallography and fractography
  - Properties of materials at low temperatures
- Read, David T.
- Physics of deformation and fracture
  - Elastic-plastic fracture mechanics
  - Mechanical properties of metals
- Reed, Richard P.
- Mechanical properties
  - Low-temperature materials
  - Martensitic transformations
- Schramm, Raymond E.
- Ultrasonic NDE of welds
  - Ultrasonic measurement of residual stress
  - Design of EMATs
- Shepherd, Dominique
- Failure analysis
  - Metallography
  - Fractography
- Shull, Peter J.
- Capacitive-array and eddy-current sensors
  - Electronics for EMATs
  - Nondestructive evaluation
- Siewert, Thomas A.
- Welding metallurgy of steel
  - Gas-metal interactions during welding
  - Welding database management
- Simon, Nancy J.
- Material properties at low temperatures
  - Database management of material properties
  - Handbook of material properties
- Tobler, Ralph L.
- Fracture mechanics
  - Material properties at low temperatures
  - Low-temperature test standards
- Walsh, Robert P.
- Mechanical properties at low temperatures
  - Mechanical test equipment
- Yukawa, S.
- Fracture mechanics
  - Codes and standards
  - Structural safety

:

# TECHNICAL ACTIVITIES



## PERFORMANCE

The Fracture Mechanics, Fracture Physics, Nondestructive Evaluation, and Composite Materials Groups work together to detect damage in metals and composite materials and to assess the significance of the damage with respect to service performance.

### Fracture Mechanics



David T. Read  
Research Leader

J. R. Berger, J. D. McColskey, H. I. McHenry, B. Petrovski,\*  
P. T. Purtscher, R. P. Reed, D. A. Shepherd, D. E. Widman,† S. Yukawa

Our research in fracture mechanics contributes to the development of fracture-prevention standards for structural materials, especially steel weldments. By using the concepts of elastic-plastic fracture mechanics, we establish material-toughness requirements, allowable stress levels, minimum service temperatures, and weld-quality standards. The quantitative methods of fracture mechanics offer advantages over the empirical methods traditionally used to develop safety standards, particularly for advanced structures where prior experience is limited.

### Representative accomplishments

- A new method, called the T-CTOD test, has been developed to locate brittle zones in steel weldments.
- The crack-driving force due to residual stresses in repair-welded steel plates has been measured using the NIST technique for direct measurement of the  $J$ -contour integral.

---

\*Guest worker from the University of Belgrade, Belgrade, Yugoslavia.

†Graduate student, Colorado State University.

- Guidelines for the assessment of pressure-vessel safety were prepared for the Occupational Safety and Health Administration. The guidelines evolved from our earlier investigation of an oil-refinery disaster.

### Local brittle zones

When we attempt to apply fracture mechanics to welded structures, material toughness data are required for comparison with the crack-driving force. Although residual stresses and material inhomogeneities cause difficulties in the calculation of the crack-driving force, the major problem is obtaining reliable toughness values. Weld-toughness testing uses specimens with precracks either in weld metal (WM) or in the heat-affected zone (HAZ). Two factors cause scatter in the results: First, the test temperature is usually in the ductile-to-brittle transition region, where scatter is high, even in base metals, because fracture initiation is governed by weakest-link statistics. Second, the welding process can produce local brittle zones (LBZ), and when the precrack tip enters a brittle zone, low toughness values result.

The HAZ is commonly reported to be the site of least toughness in a weldment. Recently, more detailed studies [Sato and Toyoda (1986); Stout et al. (1987)] of weldments for use in offshore structures have identified various microstructures within the HAZ. A high probability of brittleness was discovered for the coarse-grained HAZ microstructure.

The question of weld toughness has assumed practical importance in our study of pressure-vessel repair welding. The issues regarding driving force have been resolved to the extent that test results are sufficient for engineering applications [publication 14]. Weldment toughness, however, remains unclear. We investigated a specimen design [fig. 1, adapted from that of Kinzel (1948)] in which the crack tip samples weld metal, HAZ, and base metal in a single specimen; its descriptive abbreviation is T-CTOD, for transverse crack-tip opening displacement.

Weldments of four materials were tested using the T-CTOD specimen: 2½Cr-1Mo and 1Mn-Mo, pressure-vessel steels, a C-Mn structural steel, and a high-strength, low-alloy (HSLA) steel. The results still had considerable scatter. A key problem is the nature of the statistical weakest-link behavior; the probability of fracture depends on both the brittleness of the LBZ and the amount of the precrack front occupied by the LBZ. In the T-CTOD specimen, the weld and base metals are well-sampled, but only a few millimeters of HAZ are sampled. Thus, fracture values are scattered among values characteristic of the HAZ and values characteristic of other weld areas. A practical testing problem is fatigue-crack curvature when the strengths of the weld metal and base metal are significantly different.

Tests of T-CTOD specimens performed so far have indicated that weld metal is the most brittle site in the HSLA steel; in the three other materials, the most brittle site, apparently, is the HAZ. In the 2½Cr-1Mo steel, toughness tests indicated that the base metal adjacent to the metallographic HAZ, that is, the subcritical HAZ, is the most brittle site.

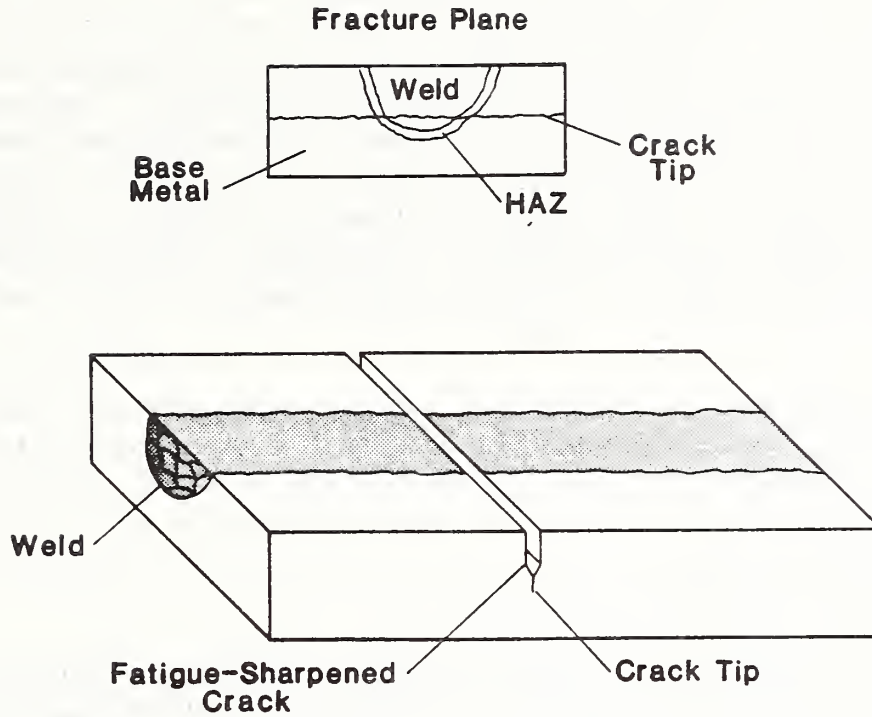


Figure 1. T-CTOD specimen.

### Surface flaws

The calculation of the crack-driving force at a surface flaw for the elastic-plastic case challenges fracture mechanics. Surface flaws are complicated because the crack-front shape and the resulting stress-strain fields cause three-dimensional effects. Approximations such as the line spring model are used to predict the general behavior of the driving force for shallow cracks in tension. The only accurate way to model the variability of the driving force along the crack front is finite-element analysis.

For cracks with this configuration, fracture initiates near the ends of the cracks. In a cooperative program with GKSS, a German national laboratory, we obtained data on five specimens of a high-strength aluminum alloy with surface cracks of various depths and aspect ratios. Because of continuing advances in applications of finite-element analysis, five reports of finite-element analyses of elastic-plastic surface cracks now exist. Because the crack geometries in the finite-element analyses differed from those in the experiments, an interpolation-extrapolation scheme was developed to relate the experimentally measured crack-mouth opening displacement (CMOD) to the  $J$ -integral at the angle of maximum crack growth,  $\theta^*$ . This involved three factors:  $CTOD(\theta = 0)/CMOD$ ;  $J(\theta = 0)/CTOD(\theta = 0)$ , and  $J(\theta^*)/J(\theta = 0)$ . Of these,  $J(\theta^*)/J(\theta = 0)$  was the most uncertain, about  $\pm 20$  percent.

We estimated  $J$  for the surface-cracked specimens, and from the fracture surfaces, we measured the corresponding crack extension,  $\Delta a$ . Then we compared these  $(\Delta a, J)$  data, which are indicative of the apparent toughness of specimen material, with values from standard testpieces. The surprising result was that the apparent toughness values at the surface cracks were 2 to 3 times higher than those of the standard testpieces. The results were the same for a second, high-strength aluminum alloy for which three surface-crack data points were available. However, in a low-strength alloy, the surface-crack data for two specimens matched the standard test-piece data.

The higher apparent toughness at surface cracks suggests the possibility of increasing the efficiency of structural components whose critical flaws are surface cracks.

### Shallow-crack fracture mechanics

As a part of the International Research Project to Develop Shallow-Crack Fracture Mechanics Tests, organized by the Edison Welding Institute, we tested specially instrumented shallow-crack ( $a/W = 0.1$ ) three-point-bend fracture specimens. The crack-mouth opening displacement at the edge of the specimens was found to be 15 percent greater than that at the center. This confirmed the finite-element analysis results of R. H. Dodds and D. T. Read [publication 13].

### Dynamic fracture analysis

In cooperation with the Department of Mechanical Engineering at the University of Maryland, stress-intensity factors for rapidly growing cracks are being calculated from strain values measured along the crack path. The procedures developed will be used to analyze data from wide plates tested by NIST in Gaithersburg for the NRC-sponsored Wide-Plate Crack-Arrest Program.

We have recently adjusted the orientation of the strain gages to  $68^\circ$  from the crack path; at this angle, the static-strain term is zero. The running crack produces a strain peak followed by a zero crossing after the crack passes. Trial tests in hardened 4340 steel specimens were performed at the University of Maryland. Plasticity effects in these specimens were eliminated to enable unambiguous comparison with calculated results, which are based on linear-elastic fracture-mechanics theory. In the development of the analysis procedure, research focuses on the need to assume constant-velocity crack propagation and the influence of higher order terms in the crack-tip strain-field expansion. Comparisons will be made of the more versatile and convenient strain-gage technique and the well-established optical technique, which uses ultra-high-speed photography to record the caustic at the tip of the running crack.

## Stretch zones

This year our study of the nature of ductile fracture in austenitic steels at cryogenic temperatures included an investigation of stretch zones. These zones can be related to fracture toughness. At cryogenic temperatures, they are characteristic of crack tips in ductile ferritic steels and aluminum, but they have not been observed in austenitic steels even though these materials are ductile in every other sense. To investigate the difference in the materials and corresponding micromechanisms, the crack-tip regions from a typical low-strength austenitic stainless steel and from a ferritic steel with a stretch zone (tested in liquid nitrogen) were examined metallographically.

The first crack growth in the austenitic steel was directly ahead of the initial crack, into an area that was not significantly deformed (or strained) prior to cracking, as shown in figure 2; therefore, no stretch zone was observed in this region. Most of the strain was absorbed in wings at 45° to the initial crack. In the ferritic steel, crack growth began at about 45° to the initial crack. The more uniformly distributed strain around the initial crack produced a blunted tip. After fracture, the stretch zone was visible on the fracture surface.

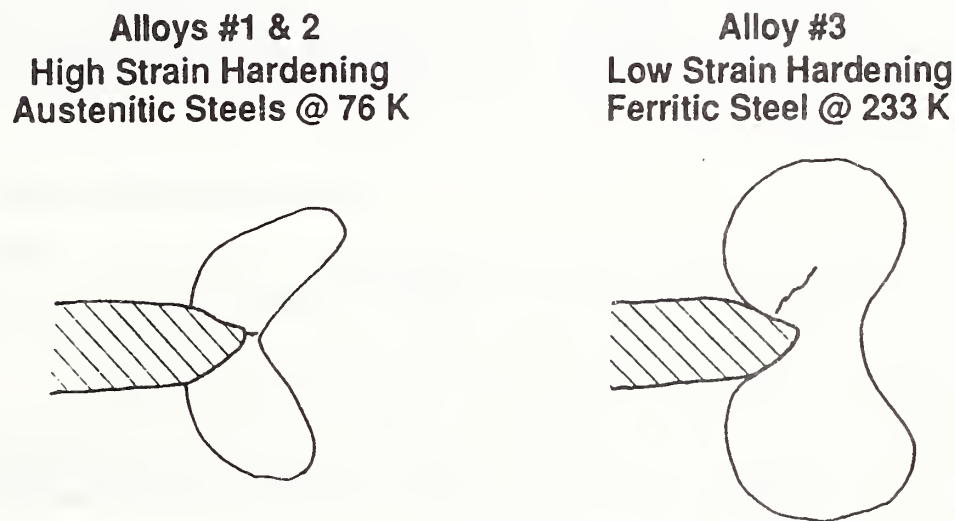


Figure 2. Highly strained zones and initial crack growth.

## Pressure-vessel safety

As a follow-up to our failure analysis of the pressure-vessel failure at a Chicago refinery in 1984, we prepared "Guidelines for Pressure Vessel Safety Assessment" for the Occupational Safety and Health Administration. It is a technical report on the design, materials, fabrication, inspection, current reliability, and damage experience for metallic pressure vessels and tanks used in general-purpose industrial applications. These vessels and tanks are usually designed and built to ASME Section VIII, Division 1 or API 620 code requirements, which are legal requirements in most places.

Several other major failures have recently occurred in tanks and pressure vessels. Inspections by vessel operators indicate that, in some environments, cracking is found in 30 to 50 percent of the vessels inspected. For non-nuclear vessels, the ASME code specifies evaluation criteria for new vessels only, not for inspection of in-service vessels. Many places have standards for repair operations, but standards for in-service inspections are rare. Vessel operators apparently are not attempting to establish such standards.

### International standards for fracture mechanics

D. T. Read participated in a task group of the International Institute of Welding (IIW) that has been working on an international standard for the application of elastic-plastic fracture mechanics. The purpose of the standard is to promote fracture-prevention measures, which are expensive, but economically advantageous in the long run.

Groups from various countries have their own approaches, and the initial attempt to adopt one of these as the international standard was not supported by delegates from other countries. The delegates thought that fracture mechanics is developing too rapidly and that applications are too varied for such an approach. Eventually, the group agreed on a different strategy: rather than establishing a standard method for performing a fracture-mechanics assessment, they established a standard method for reporting the assessment. The proposed document

- presents an introduction to the basic principles of fracture mechanics
- briefly describes all known current methods
- includes sample problems with solutions and comments
- requires that specific technical information be included in the report to enable verification of its nature and quality

The IIW plans to advance this document, along with companion parts on different aspects of structural safety, to the International Standards Organization (ISO) as an international standard.

### References

- Kinzel, A. B. (1948). Ductility of steels for welded structures. *Weld. J. Res. Suppl.* 27: 217s-234s.
- Sato, K.; Toyoda, M. (1986). Guideline for fracture mechanics testing of WM/HAZ. Document X-1113-86. Tokyo: International Institute of Welding.
- Stout, R. D. et al. (1987). *Weldability of Steels*. New York: Welding Research Council. 298-300.

## Fracture Physics



Ing-Hour Lin  
Research Leader

V. Tewary,\* R. M. Thomson†

Research of the Fracture Physics Group is directed toward understanding (1) the fracture of materials in terms of their fundamental properties and the interactions between cracks and dislocations and (2) the effects of external chemical environments on cracks in brittle materials. Many of our studies model dislocation emission from sharp cracks and the influence of dislocation shielding on material toughness.

### Representative accomplishments

- A new model attributes cleavage initiation in steels to inclusions on the cleavage plane, which suppress dislocation emission at the crack tip.
- Relativistic equations that govern crack shielding in dynamic fracture were developed to explain why the plastic zone size decreases with crack velocity at a given static stress-intensity factor.

### Activation-energy calculations for dislocation emission from a crack in silicon

Recent studies have indicated that previous estimates by J. Rice and R. Thomson (RT) (1974) of the activation energy for emission of dislocations from crack tips are probably too high for many materials, and also that nonblunting dislocation configurations are usually observed, rather than dislocations that blunt the crack. In this study, we made a series of calculations for silicon. One configuration was split into

---

\*Visiting scientist from Ohio State University, Columbus, Ohio.

†Institute Scientist, Institute for Materials Science and Engineering.

partial dislocations, whose stacking-fault energy value was determined by P. Haasen (1983). The activation energy was, indeed, much less than that in the original RT estimate. The lowest energy configuration, obtained by using a two-dimensional estimate of the image term (similar to that used in the RT estimate) is a blunting half-loop, but the three-dimensional image contribution shifts the result toward lowering the energy of the nonblunting configuration relative to the blunting case.

### Effects of plate-like rigid inclusions on the ductile-brittle transition

We have proposed a simple model of dislocations, cracks, and inclusions to study inclusion embrittlement in steels [publication 32]. The elastic interactions among screw dislocations, a plate-like rigid inclusion, and a crack under antiplane shear strain, as shown in figure 3, were derived and applied to a study of dislocation emission at crack tips and crack-tip breakaway from shielding dislocations. Our results suggest that the stress-intensity factor required for emitting a dislocation at a crack tip increases, and the intrinsic character of cracks changes from ductile to brittle when a plate-like rigid inclusion is on the cleavage plane and very close to the crack tip. Furthermore, the inclusion-induced cleavage fracture triggered by void nucleation at the inclusion was analyzed qualitatively to account for the fracture toughness in steel, which decreases with an increase in the volume fraction of inclusions.

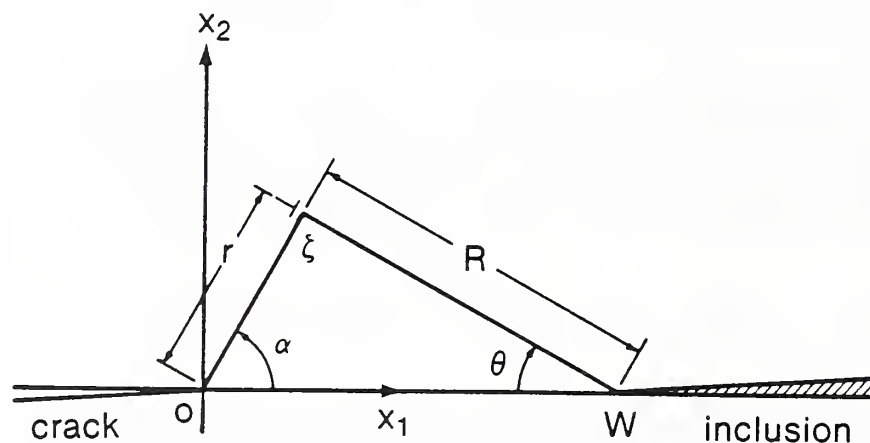


Figure 3. Coordinate system for dislocation-crack-inclusion interactions. The crack tip is at the origin with the cleavage plane along the negative  $x_1$  axis. The inclusion is along the positive  $x_1$  axis with its tip at  $x_1 = w$ . The dislocation is at  $\zeta$ , measured from the crack tip.

## Crack shielding in the context of a composite

During interlaminar failure of a brittle polymer-matrix composite in which the crack lies parallel to the fiber direction, there is an elastic interaction between the fiber and the crack that can be analyzed by using previously developed ideas for crack shielding by dislocations. We have developed an analysis along these lines, modeling the fibers as line forces and line-force multiples, which indicate the shielding and antishielding. We also investigated the branching forces on the crack due to the fibers. Somewhat different concepts apply to ductile polymer-matrix composites, and in this case, we shall develop a shielding model based on the Bilby-Cottrell-Swinden (BCS) theory.

### Dynamic-fracture toughness

To develop the relativistic equations that govern crack shielding, we took the one-dimensional BCS model [modified by S. J. Chang and S. M. Ohr (1981)], which serves as a zeroth-order approximation for all dislocation crack-shielding modeling, and generalized it to steady-state relativistic velocities [publication 33]. This crack shielding is illustrated in figure 4. Later, we shall pursue the consequences of dislocation-free zones and ligament shielding for fast fracture and arrest and compare such models with the continuum-based case. Although some controversy exists about the presence of dislocation-free zones and the role they play in fracture, we think that they should not be ignored in modeling the crack-tip behavior. In particular, we think that the fracture toughness laws for fast crack growth and arrest should incorporate ideas about the dislocation-free zone in order to ensure that the proper physics of the crack-dislocation interactions has been incorporated into the final models.

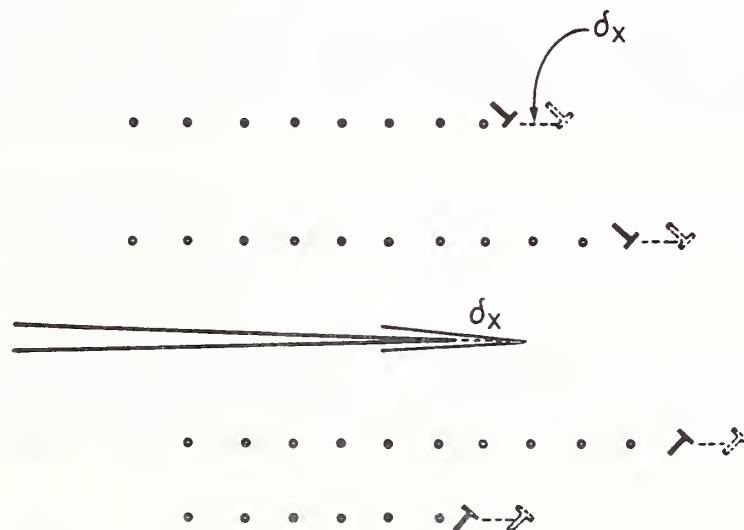


Figure 4. Moving crack with self-similar shield and wake. For a moving crack in the steady state, we assume that a self-similar shield is generated at each position and the energy of moving this shield is equivalent to creating a wake for each dislocation in the shield.

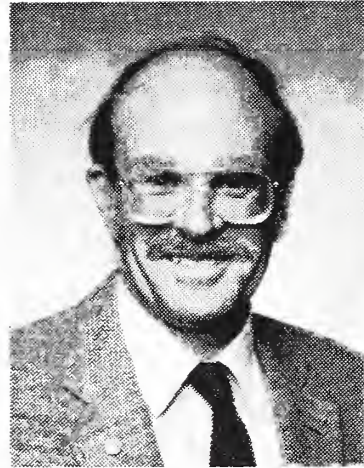
## The chemical wedge in brittle fracture

A new theory has been developed for the observed activated crack growth that incorporates the discrete effects at the crack tip with the long-range surface forces. When external chemical environments are present during fracture, one of the issues that must be settled is whether the external molecules reach the crack tip. If the external molecules do not reach the tip, then any activated crack growth observed is due to molecular transport through the near-tip region, rather than to stress-assisted chemical reactions. It turns out that the criterion for reaching the tip is complicated in the case of molecules that are large compared with the crack-tip opening at the relevant stress-intensity level. Suppose, for example, that the molecules are large and that a region exists near the crack tip from which they are excluded because of their size. Since the surface area covered by the external molecules has a surface energy different from that just ahead of the last molecule (wedge tip), a surface tension operates on the wedge tip that tends to draw the molecules further into the crack-tip region. As this happens, the molecules push the walls of the crack open, thus generating compensating elastic-configuration forces on the molecular wedge. When the surface tension force is equal and opposite to the elastic forces exerted by the walls, the wedge comes into a Griffith-type equilibrium. We have carried out detailed atomic calculations based on lattice Green's functions for the case of water interacting with a crack in mica.

## References

- Chang, S. J; Ohr, S. M. (1981). Dislocation-free zone model of fracture. *J. Appl. Phys.* 52: 7174.
- Haasen, P. (1983). Electronic processes at dislocation cores and crack tips. Latanision, R. M.; Pickens, J. R., eds. *Proceedings of a NATO Advanced Research Institute on Atomics of Fracture*. New York: Plenum. 707.
- Rice, J.; Thomson, R. (1974). Ductile versus brittle behaviour of crystals. *Philos. Mag.* 29: 73.

## Nondestructive Evaluation



Alfred V. Clark, Jr.  
Group Leader

D. W. Fitting, D. V. Mitraković,\* R. E. Schramm, P. J. Shull

Our Nondestructive Evaluation (NDE) group develops measurement methods and sensors for evaluating the properties and the processing of materials. To improve structural safety, we use electromagnetic acoustic transducers (EMATs) to detect and size flaws and to measure residual stresses. For advanced materials, we develop sensors to monitor elastic property degradation in polymeric composites, sintering of ceramics, curing of polymers, and crystalline texture formation in steel sheet.

### Representative accomplishments

- Acoustical arrays of piezoelectric polymer elements were developed to measure elastic-wave propagation in composites.
- Capacitive array probes, which are sensitive to the change in dielectric constant during material processing, successfully monitored the cure of a polymer-matrix composite.
- A flaw detection system for railroad wheels was developed for use in a roll-by mode. EMATs were mounted inside a cavity in a railroad track and automatically pulsed when a railroad wheel was on top of it.
- Proof-of-concept experiments were conducted for a nondestructive, on-line formability sensor. Ultrasonic velocity measurements related to crystalline texture correlated well with destructive measurements of formability.

---

\*Guest worker from the University of Belgrade, Belgrade, Yugoslavia.

## Acoustical arrays

Acoustical arrays were constructed from a piezoelectric polymer and polyvinylidene fluoride. Because the array elements are smaller than the acoustical wavelength used, the output of the array is less affected by artifacts than the output of a conventional acoustical transducer, which averages the signal over the entire transducer aperture. The output of the acoustical arrays is broadband—200 kHz to 35 MHz. Measured electrical and acoustical crosstalk (interference between adjacent array elements) is small (about 1 part in  $10^3$ ). Because each array element is omnidirectional, the array can be steered; that is, by suitably delaying the output of each array element, the array can be made more responsive to signals arriving from a chosen direction.

A promising use for acoustical arrays is the characterization of composite materials, such as graphite/epoxy panels. The basic concept is illustrated in figure 5: a receiving array detects an ultrasonic wave propagating at an angle to the graphite fiber direction. By measuring phase velocities at different angles to the fiber directions and using the known relation between the composite elastic moduli and phase velocities, the elastic properties can be obtained.

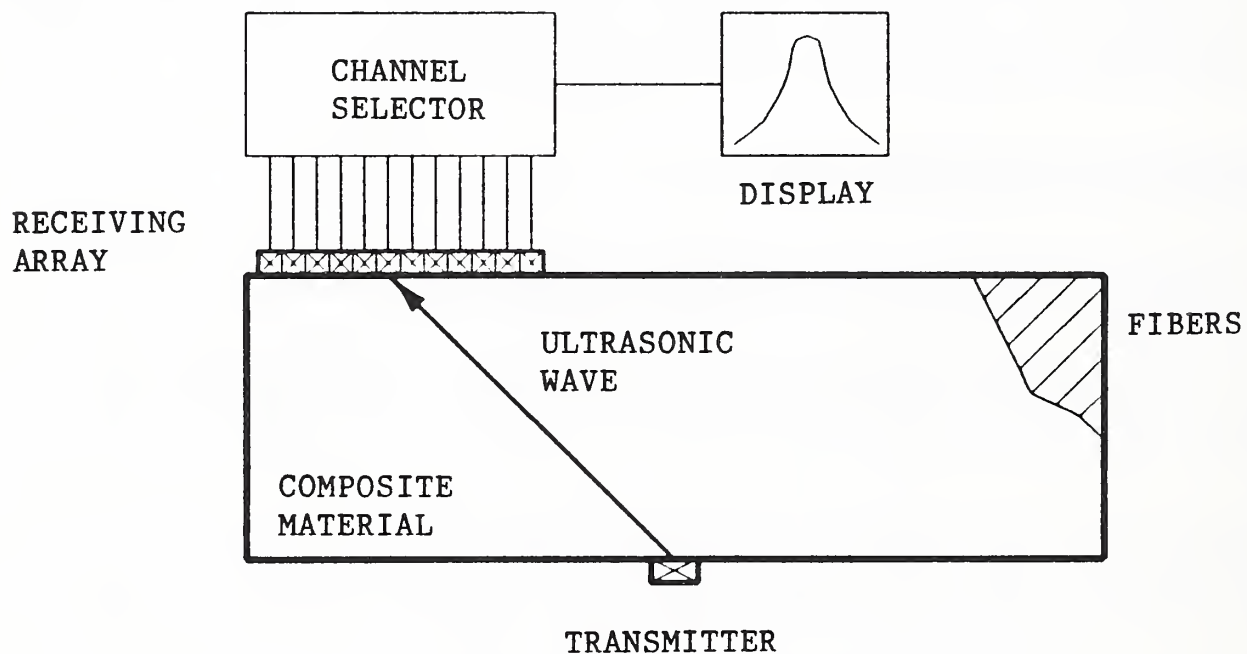


Figure 5. Basic concept of acoustical arrays.

Composite materials have a peculiarity not found in isotropic materials, such as metals. Because composites are anisotropic, the direction of energy-flux propagation will not usually coincide with the normal to surfaces of equal phase in the acoustical beam, as shown in figure 6. The transmitting transducer, *T*, generates two beams, marked *QL* and *QT* (quasi-longitudinal and quasi-transverse); each beam propagates its energy as

shown by the arrows. The surfaces of equal phase are normal to the wave vector. In the QL beam, the particle motion is predominantly perpendicular to the specimen surface; in the QT beam, the particle motion is predominantly tangential. In contrast, in an isotropic material, only one beam propagates; it propagates along the wave-vector direction with particle motion perpendicular to the surface.

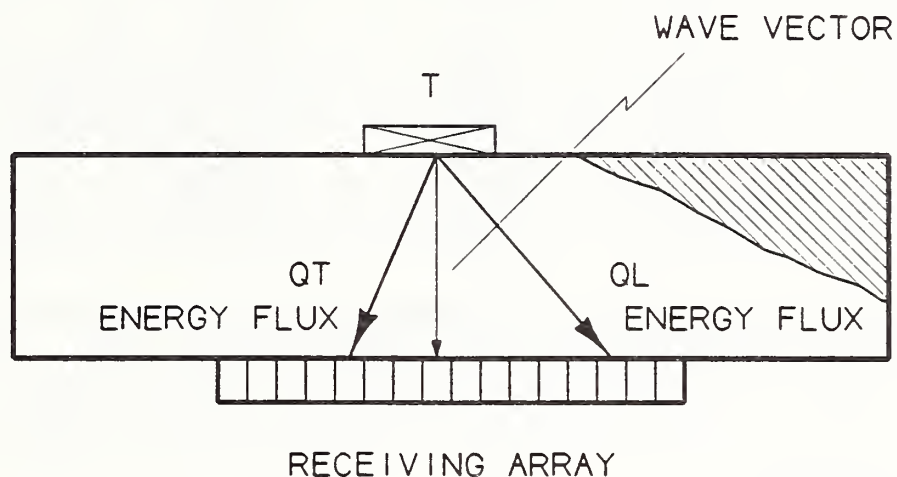


Figure 6. Measurement of energy-flux direction and arrival time in sectioned samples of a unidirectional composite.

Thus, to determine the elastic properties in a composite material, it is necessary to

- a. scan the array elements to determine where the QL and QT beams arrive
- b. record the arrival time of these beams
- c. divide the times by specimen thickness to obtain an equivalent velocity for each beam
- d. perform an inversion to obtain elastic properties from arrival times

To validate the above procedures, proof-of-concept experiments were performed. Specimens of a unidirectional graphite/epoxy panel were cut at different angles to the fiber direction. In the experiments, the arrays were fixed in place and scanning was done by multiplexing the array (addressing each element in sequence).

From the known elastic properties of the constituents (graphite and epoxy) and the computed centroids of the measured beams, the energy-flux deviation was calculated for each specimen. Flux deviation was measured for the QL and QT beams and compared with the calculated predictions. Typical results for the QL wave summarized in Table 1 show that good overall agreement was obtained.

Table 1. Comparison of Energy-Flux Directions of QL Waves

Fiber Angle	Bulk Wave Predicted	Scanned Receiver	Array Centroid of Measured Amplitude
28	26.4	24.1	26.4
28	26.4	24.1	26.0
45	42.1	42.0	40.4
45	42.1	43.3	44.2
55	50.7	50.8	50.1
70	60.8	57.6	57.4

NOTE: All entries are in degrees.

### Capacitive array probes

Work on the use of capacitive array probes for materials characterization continues [publication 63]. Current research focuses on two applications: monitoring the sintering of ceramics and monitoring the cure state of polymeric composites. In both cases, the dielectric constant of the material changes during processing. The capacitive probe is sensitive to the dielectric constant of material in the vicinity of the probe, so the probe should be a good process monitor.

The principle of probe operation is illustrated in figure 7a. A voltage is placed across two electrodes, and the resulting electric field between the electrodes is as shown. The field is most intense close to the electrodes and decays with distance. The field can be modified by changing the electrode configuration, as shown in figure 7b. Here, two electrodes are at a high potential ("source" electrodes) and two are at a lower potential ("receiver" electrodes). The resulting electric field is more intense between the electrodes and spreads farther from the electrodes.

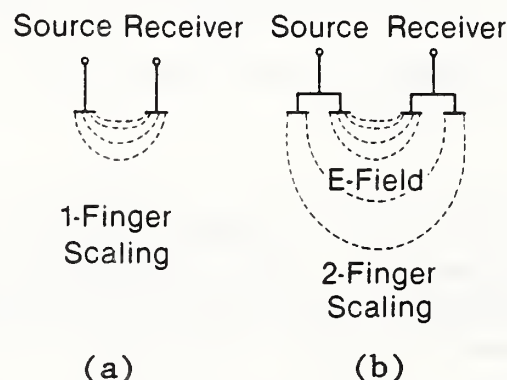


Figure 7. Principle of probe operation.

Measurements of probe admittance can be made to characterize material in proximity to the probe. The admittance is the ratio of current flowing in the receiver electrodes divided by the potential difference. The admittance is affected by the material dielectric constant,  $\epsilon$ , and by the distance,  $d$ , to the specimen surface.

In our work on sintering of ceramics, we have constructed probes of different geometries and tested them on a variety of ceramics with different  $\epsilon$ . Our initial idea was to multiplex the electrodes to vary the probe's electrical geometry and to use an elementary theory to predict both  $\epsilon$  and  $d$  from our admittance measurements. Initial measurements did not agree with theoretical predictions. After numerous experiments using several probes on materials with a range of  $\epsilon$ , we discovered that one artifact was caused by (a) the way our instrument measures admittance and (b) parasitic coupling of electrical flux to ground points in the probe environment.

Having identified sources of experimental error, we were able to suppress some artifacts. For example, a specimen was placed atop a ground plane, which is an aluminum sheet. Current in the sheet was added back into the impedance analyzer, along with the receiver current. The result is shown in figure 8 along with theoretical results. Good overall agreement was obtained.

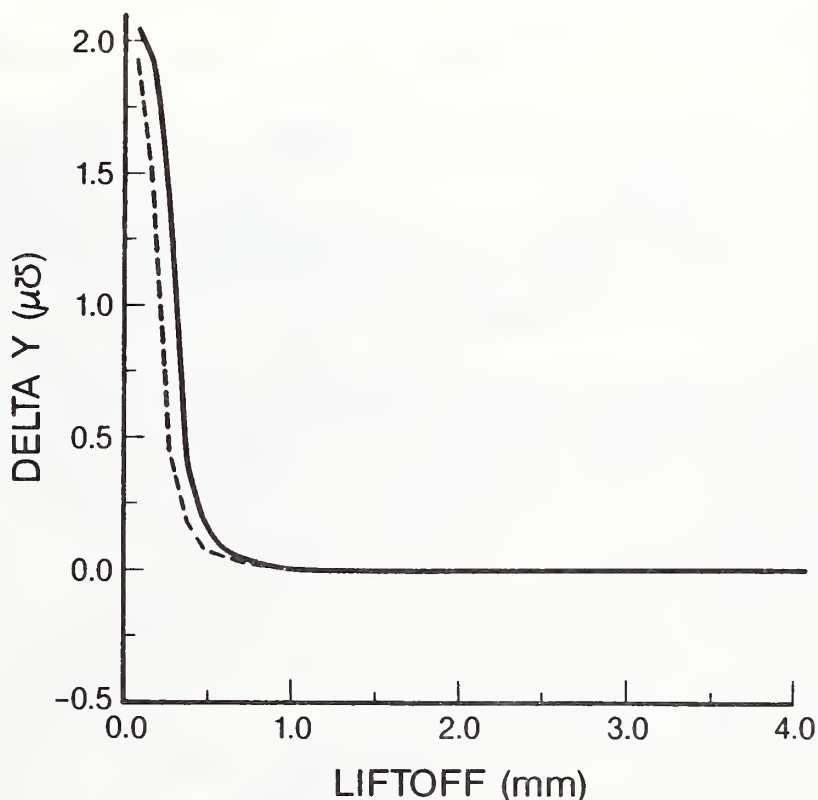


Figure 8. Comparison of theoretical (broken line) and experimental (solid line) liftoff response for the capacitive array.

Monitoring the cure of graphite/epoxy composites is based on changes in conductivity,  $\sigma$ , and dielectric constant,  $\epsilon$ , with cure state. In general, the composite's conductivity dominates the dielectric effect for the frequencies used in our experiments (in contrast with the ceramics case, where conductivity is negligible). Consequently, an initial concern was that composite conductivity would blind the probe to changes in electrical properties within the specimen.

Proof-of-concept experiments showed that the probe can indeed follow the cure of a composite. A thin film of commercial, fast-setting epoxy was placed atop a 6-mm-thick unidirectional plate of cured graphite/epoxy. The panel was, in turn, placed atop the capacitive array probe. The magnitude and phase of the receiver-electrode current were measured as a function of time. As seen from the results in figure 9, the probe was indeed sensitive to the cure state.

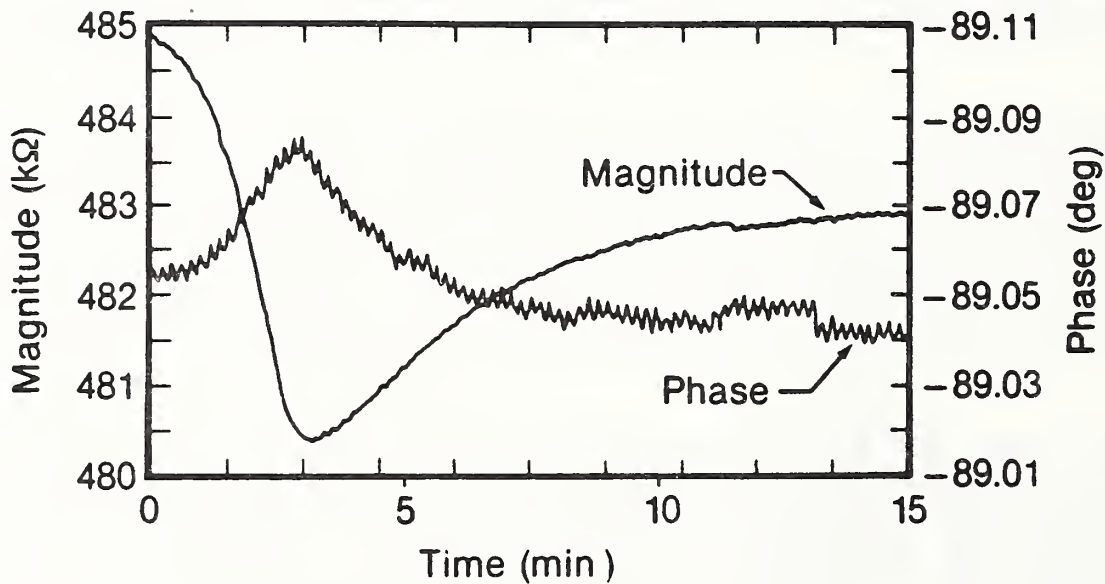


Figure 9. Magnitude and phase of the receiver-electrode current.

Measurements were repeated with variations in operating frequency and probe spatial frequency. As the operating frequency was decreased from 100 kHz to 1 kHz, the phase changed more with time. This is in qualitative agreement with theory, which predicts a greater sensitivity to conductivity at lower operating frequencies. As the spatial frequency was decreased, electromagnetic field penetration of the composite increased, and greater sensitivity to curing was observed, again in qualitative agreement with theoretical expectations.

## Electromagnetic-Acoustic Transducers

### A. *Evaluation of defects in railroad wheels in a roll-by mode*

Our nondestructive evaluation of railroad wheels moved forward with the receipt of sections of rail and several wheel sets (two wheels mounted on an axle). We constructed a short "railroad" from the rails and mounted the wheel set on the tracks; see figure 10. With the laboratory-size railroad, we were able to develop a technique to detect and evaluate defects in the wheels as they rolled over the track.

In previous work, electromagnetic-acoustic transducers (EMATs) were placed directly on the wheel tread to interrogate artificial defects (saw cuts) [publications 9, 58, 59]. In the laboratory railroad, an EMAT was mounted in a small cavity that we had machined into the rail. The wheel set was positioned so that one wheel was directly over the EMAT, and signals reflected from defects were compared with those of the EMAT placed directly on the wheel. Because the efficiency of EMAT signal generation is very sensitive to liftoff (distance from EMAT to tread), we were concerned about how well the EMAT would perform in the rail. Preliminary experiments indicated that, by backing the EMAT coils with a flexible substrate to minimize liftoff, a good signal-to-noise ratio could be achieved with the EMAT in the rail.

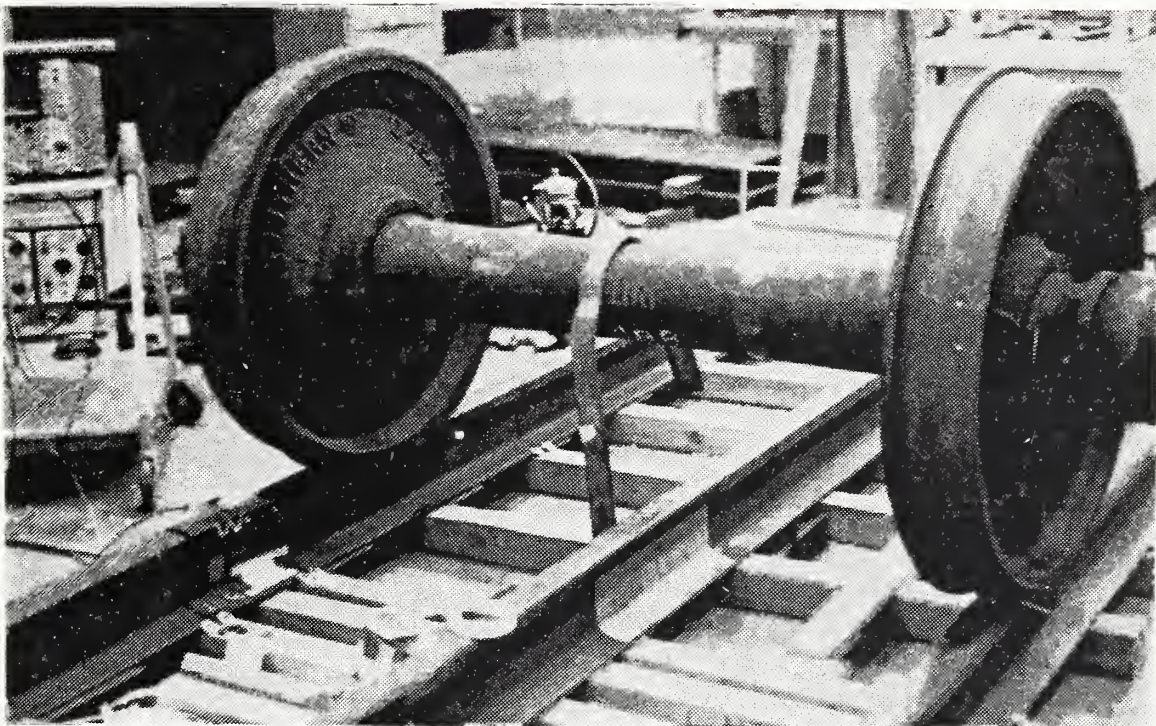


Figure 10. Laboratory-size railroad.

The above experiments were performed in a static mode, that is, with the wheel positioned directly over the EMAT. Next, a simple trigger was constructed that caused the EMAT to be pulsed when the wheel was atop the EMAT. Simple roll-by tests were then performed. The wheel was propelled by hand over the EMAT; the trigger caused the EMAT to generate and receive signals in the tread as it passed by. These signals (captured on a high-speed transient recorder) compared favorably with those observed in the static mode.

The transmitting EMAT coil was redesigned so that it generates the same signal amplitude, but requires a lower drive current; it is identical to the wire-wound receiving unit. The new EMAT is more reliable, and the life of the MOSFET output stage in the pulser has been increased. Also, should it be necessary, the pulser's repetition rate can be increased.

The parameters limiting train speed are: (a) pulse-repetition frequency, (b) signal-processing time requirements, and (c) distance between wheels on a railroad truck. The maximum roll-by speed appears to be about 40 km/h (25 mph), but it is subject to further testing and development.

#### *B. Ultrasonic measurement of steel-sheet formability*

Previous research has focused on ultrasonic measurement of texture and formability in aluminum alloy sheet [publications 6-8]. During the past year, the focus shifted to steel. In this effort, we are collaborating with the Advanced Steel Processing and Products Research Center (ASPPRC) at the Colorado School of Mines and interacting with researchers in the automobile and steel industries.

A prototype ultrasonic system was developed and demonstrated to industrial sponsors of the ASPPRC. Their response was favorable because

- a. current methods of characterization of steel-sheet formability are destructive;
- b. these methods are time-consuming;
- c. they cannot be implemented in applications such as a rolling mill or press shop;
- d. the NIST prototype system has the potential to overcome all the above objections.

A block diagram of the ultrasonic system is shown in figure 11. The function generator delivers a high-frequency signal to a high-current pulser. The pulser can deliver short-duration current pulses of up to 150 A into a load that is tuned with the impedance-matching circuit. The transmitting EMAT generates a wave that is guided by the plate and detected with the receiving EMAT. The output of the receiving EMAT goes through a special matching network and into a low-noise, high-gain amplifier. The amplified output is in the form of a sine wave of finite duration. The digital-gate and comparator circuit selects a zero crossing (a time when the voltage is zero) in the wave and stops the counter at that point. The counter has been running continuously since receiving a trigger signal coincident with the firing of the current pulse.

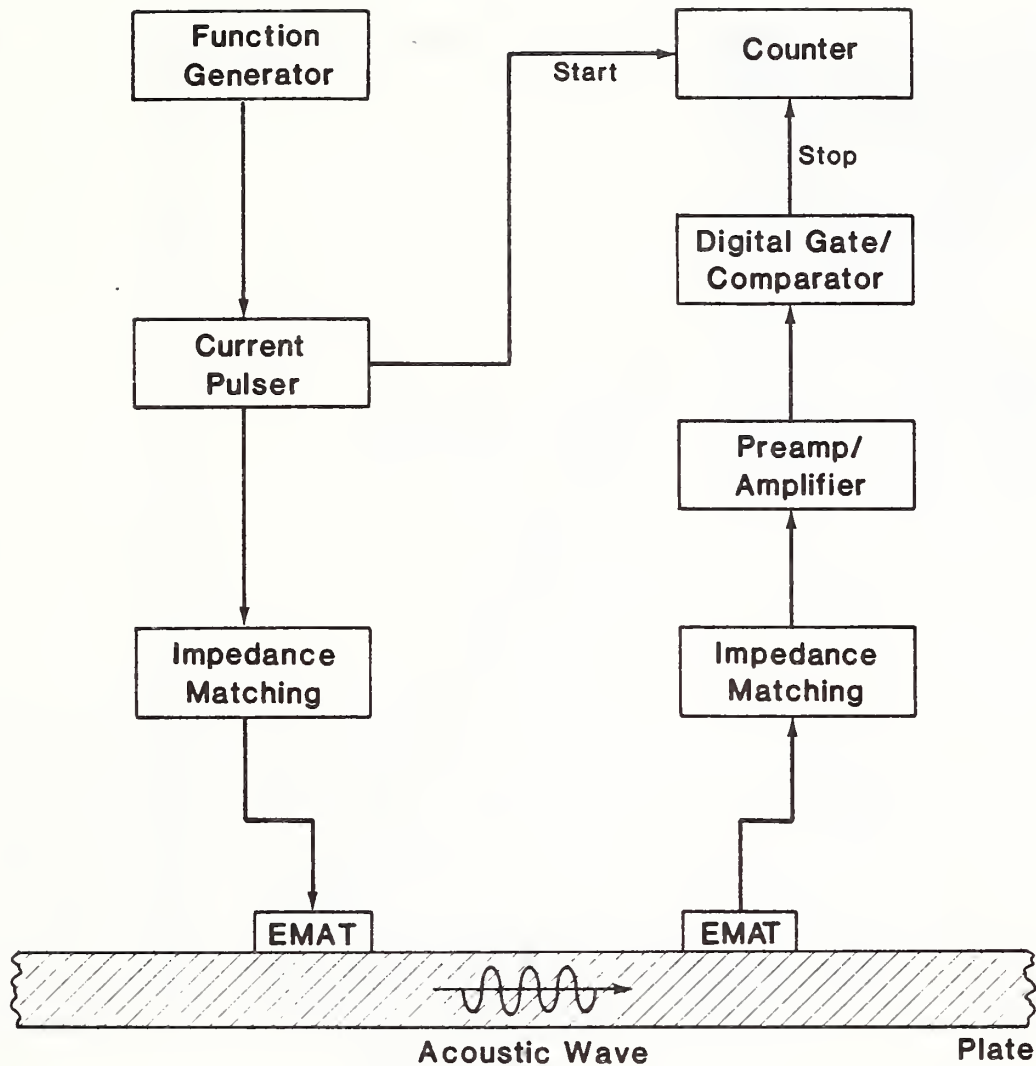


Figure 11. The ultrasonic system

The system was used to measure combinations of arrival times of guided waves traveling at different angles relative to the sheet rolling direction. These measurements were done on low-carbon steel sheet typically used for automobile bodies. Destructive measurements of the average formability,  $\bar{r}$ , of these sheets had been made by the supplier.

A comparison of  $\bar{r}$  with  $\langle T_{SO} \rangle$  is shown in figure 12; here,  $\langle T_{SO} \rangle = (1/4)[T(0^\circ) + T(90^\circ) + 2T(45^\circ)]$ , where  $T(\theta)$  is arrival time of the guided wave traveling at angle  $\theta$  to sheet rolling direction. As can be seen from figure 12, good agreement was obtained between ultrasonic and destructive formability measurements for a relatively small data set. Measurements on a larger set of sheets supplied by a major automobile manufacturer are currently under way. These sheets are typical of those used in press-shop operation.

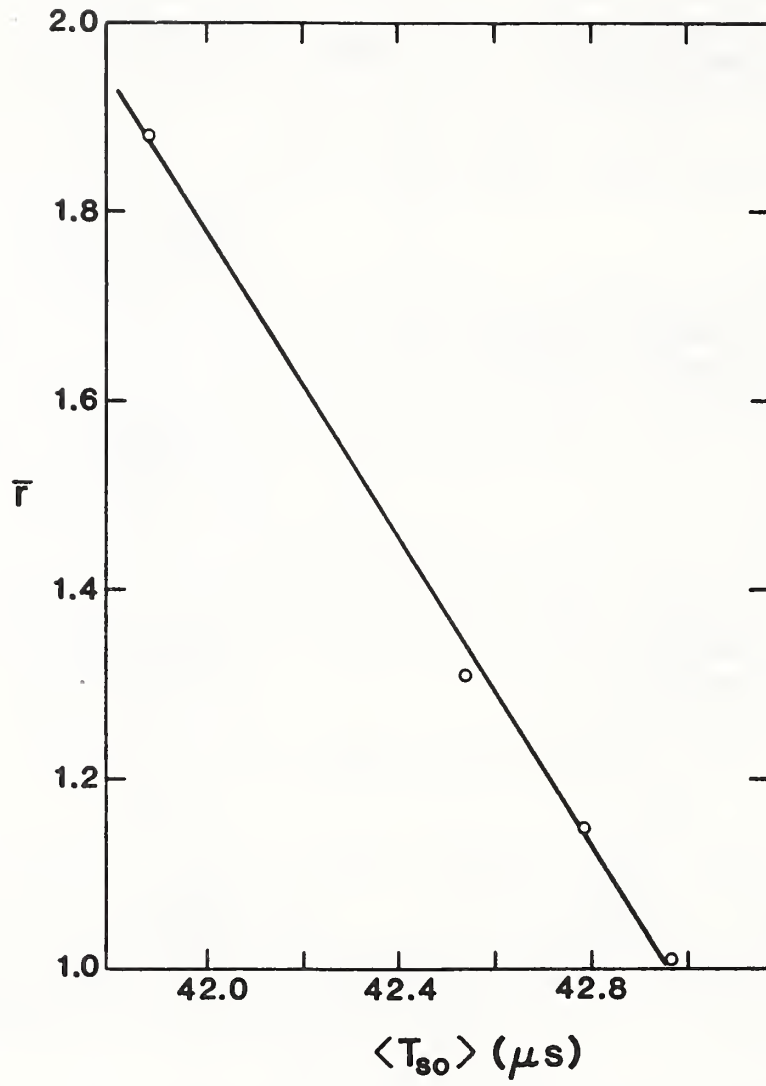
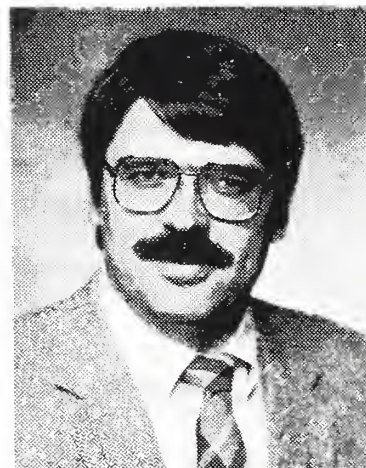


Figure 12. Comparison of ultrasonic and destructive formability measurements.

## Composites



Ronald D. Kriz  
Research Leader

M. W. Austin, J. R. Berger, P. R. Heyliger, J. D. McColskey, V. Tewary\*

Our research in composites emphasizes (a) the mechanics of fracture and (b) the mechanics of nondestructive evaluation of particulate and fiber-reinforced structural laminates. Our approach to these topics is both analytical and experimental. Unlike conventional homogeneous isotropic materials, fiber-reinforced composites can be designed for specific applications by controlling their wide range of parameters, which include fiber volume fraction, fiber orientation, interface properties, laminate stacking sequence, and fiber-matrix elastic properties. We study how these design parameters relate to the mechanical performance of selected composites.

### Representative accomplishments

- The accuracy of strain measurements made with an optical strain diffractometer has been increased by a factor of 50. A manual system using one camera has been replaced by an automatic system using four cameras. Thirty-seven times more area can be scanned in one-twelfth the time.
- For the first time, the deformation topologies of stress waves propagating in graphite/epoxy materials have been calculated using finite-element analysis (FEA). Previously predicted columnar wave structures and mode transitions in displacement fields have been substantiated with FEA.

---

\*Visiting scientist from Ohio State University, Columbus, Ohio.

## Composite fracture mechanics

Fracture mechanics is not as well established for composites as it is for homogeneous isotropic materials. Therefore, we have been developing new analytical and experimental methods to understand the physical significance of different kinds of damage in laminated composites (i.e., ply cracks, interface cracks, delaminations, edge stresses). For sponsors, we have measured the mechanical properties of new materials that are candidates for specific applications.

### A. Analytical methods for calculating singularities in laminates

As part of a long-term project, we are studying new methods to predict three types of singularities (fig. 13) at bimaterial interfaces in laminated structural composites.

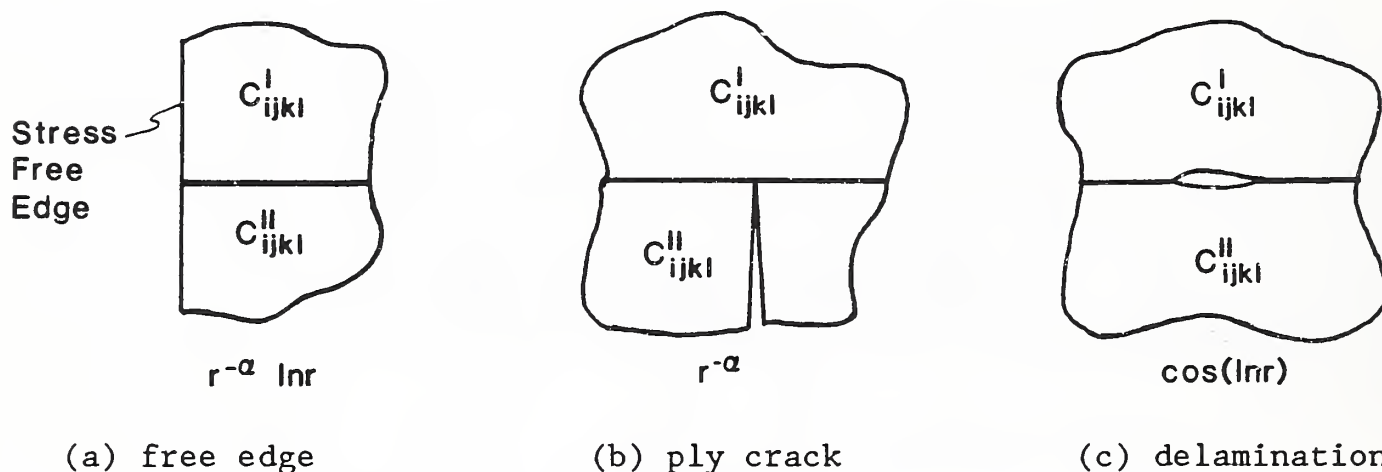


Figure 13. Types of singularities at anisotropic bimaterial interfaces.

We are using Stroh's method to evaluate the free-edge and ply-crack singularities. We intend to study the delamination singularity by a Green's function method that has recently been developed in our division. For the three types of singularities, the total boundary-value problem is solved numerically: enriched finite elements are used to model the near-field singularities, and the coefficients of these singular terms are calculated by the conventional finite-element-displacement method.

### B. New composite materials for thermal-isolation straps

Thermal isolation straps are used in satellites, where long-term containment of cryogenics is required for sensor cooling. In an earlier program [publication 21], we evaluated glass-fiber-reinforced epoxy (G1/Ep) material for this application. Subsequently, it replaced aluminum-oxide-fiber-reinforced epoxy ( $\text{Al}_2\text{O}_3/\text{Ep}$ ) because its properties were superior:

lower thermal conductivity and higher stiffness and fatigue life. Recently, we tested the mechanical and thermal performance of an improved material ( $\text{Al}_2\text{O}_3/\text{PEEK}^*$ ). Properties determined from mechanical tests for tension, compression, and in-plane shear were similar to those of  $\text{Al}_2\text{O}_3/\text{Ep}$ , but the thermal conductivity measured by L. Sparks and D. Rule† was substantially better than that of  $\text{Al}_2\text{O}_3/\text{Ep}$  (see fig. 14).

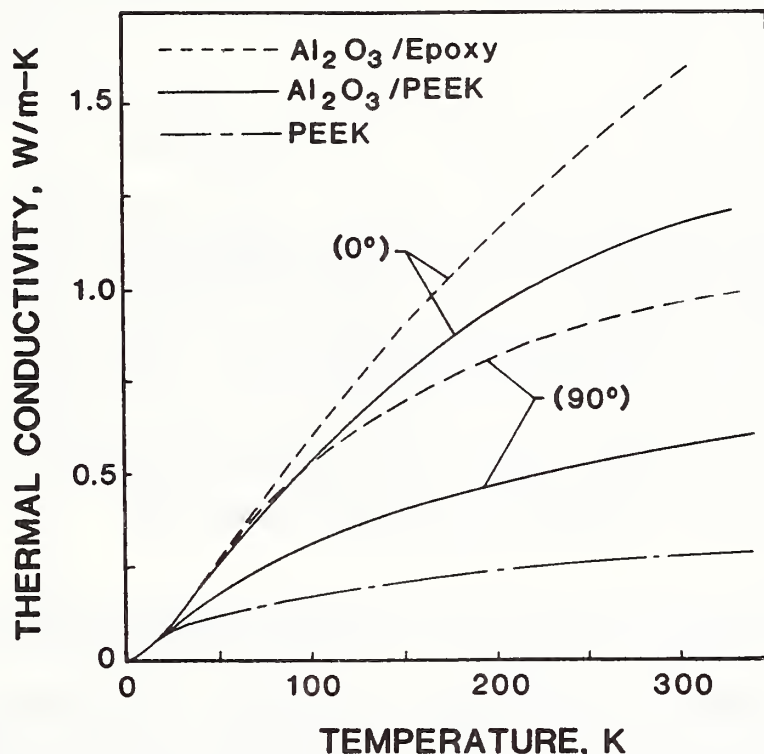


Figure 14.  $\text{Al}_2\text{O}_3/\text{PEEK}$ ,  $\text{Al}_2\text{O}_3/\text{epoxy}$ , and neat PEEK, parallel ( $0^\circ$ ) and perpendicular ( $90^\circ$ ) to the fibers.†

Although quasi-static mechanical tests showed no improvement of  $\text{Al}_2\text{O}_3/\text{PEEK}$  over  $\text{Al}_2\text{O}_3/\text{Ep}$ , we think that improved fatigue life of the thermal isolation straps is possible. Because of the high strain-to-failure properties of the  $\text{Al}_2\text{O}_3$  fibers,  $\text{Al}_2\text{O}_3/\text{Ep}$  is particularly suitable for filament winding. Unfortunately, the manufacturer encountered many processing problems in filament winding the fatigue straps fabricated from  $\text{Al}_2\text{O}_3/\text{PEEK}$ . Hence, fatigue tests have been indefinitely postponed pending further research. We think further research is warranted because of the low thermal conductivity of the material.

\*PolyEther-Ether-Ketone.

†Properties of Solids Group, Center for Chemical Engineering, National Institute of Standards and Technology.

### C. Mechanical tests of graphite-fiber-reinforced PEEK

In an aerospace application, graphite-fiber-reinforced PEEK (Gr/PEEK) is being considered as a lightweight material for the containment of liquefied gas fuels. Our division received a contract to measure its mechanical properties at cryogenic temperatures. Preliminary results indicate adequate strength, stiffness, and bond strengths for the intended application. Here, Gr/PEEK is superior to  $\text{Al}_2\text{O}_3/\text{PEEK}$  because of its higher specific strength and stiffness.

### Mechanics of nondestructive evaluation for composites

Our nondestructive evaluation (NDE) studies concentrate on (a) measuring and mapping the mechanical deformation near damage in a composite laminate with optical diffraction techniques and (b) developing a numerical model to predict the full-field deformation topologies of stress waves propagating through an off-axis unidirectional graphite/epoxy composite. Both efforts emphasize modeling the *mechanics* of deformation as it relates to damage in a quasi-static state of deformation and as it relates to the dynamic deformation of a propagating stress wave. Both topics address mechanics of deformation together with a commonly used NDE technique.

#### A. Determination of strain fields in damaged composite panels

Because damage in composite structural laminates is heterogeneous, an inhomogeneous distribution of strains corresponds to the growth of this damage. To map the distribution of this heterogeneous strain field, the NIST optical strain-measurement technique [Moulder et al. (1986)] has been improved. With this technique, we shall study the initiation and growth of impact damage in structural laminates with emphasis on the relationships between the damaged strain regions and laminate structural performance.

Several improvements have been realized on the NIST optical strain-measurement technique. Briefly, it uses the optical diffraction of a coherent light source to measure localized strain over a portion (i.e., 1-mm diameter) of a deformed Moiré grid, which is attached to the surface of a specimen while under load. Strain is calculated from changes measured in the diffraction pattern, which correspond to in-plane deformation of the Moiré grid.

More accurate strain measurements were obtained by measuring small displacements of the four first-order diffraction dots. This is accomplished by calculating the centroid of the intensity of each of the four (north, south, east, west) diffraction dots. Each diffraction dot is resolved with a CCD camera ( $512 \times 488$  pixels); standard image-processing hardware and software for personal computers are used. A sample of diffraction dot intensity is shown in figure 15, where the useful portion of a diffraction dot is resolved over approximately 80-pixel diameter.

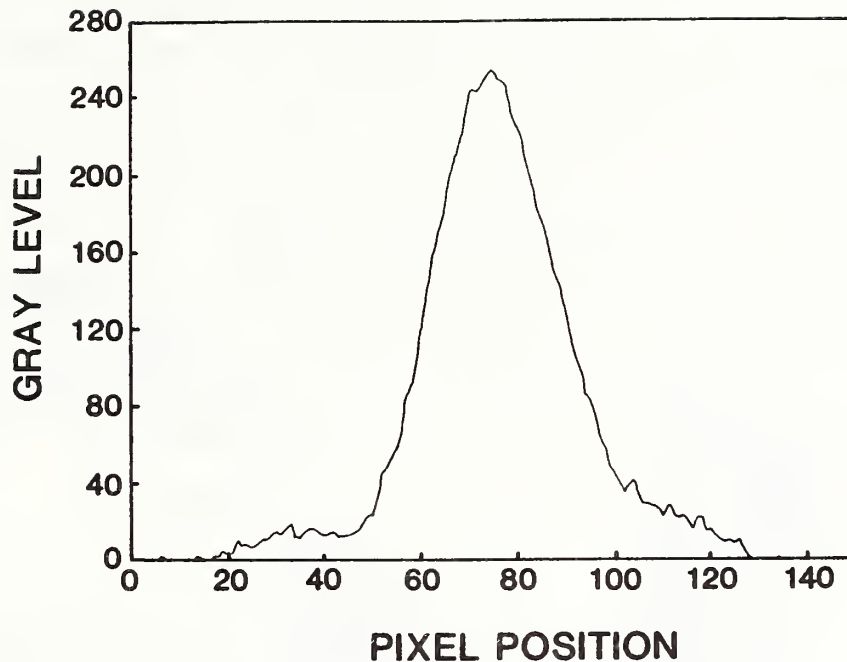


Figure 15. Intensity profile of first-order diffraction dot.

Each diffraction-dot centroid has been resolved within 1/1000 of the pixel dimension, which translates into a strain accuracy of  $\pm 100 \mu\epsilon$ . (The previous system accuracy was  $\pm 5000 \mu\epsilon$ .) The resolution has also been improved by automating the position control, which is used to scan the deformed Moiré grid, and the image-processing system from the sample-compiled program. The previous manual system mapped only a small area ( $21 \times 21$  pixels) in three days. The automated system maps a larger area ( $128 \times 128$  pixels) in six hours.

#### *B. Stress-wave topologies in off-axis graphite/epoxy composites*

The topological propagation of stress waves in off-axis unidirectional fiber-reinforced composites were modeled with finite elements [publication 15]. Solutions for the large finite-element grids were obtained in reasonable times by using the large memory and vectorizable features of the NIST mainframe computer. In a unidirectional graphite/epoxy plate, waves propagate off the fiber axis. Wave speeds and propagation directions were predicted by finite-element analysis and compared with those predicted by Christofel's equation (plane stress and plane strain were assumed). The agreement was excellent. Most significant were the actual deformation topologies of the quasi-transverse and quasi-longitudinal waves; the geometric distribution of these columnar wave structures are demonstrated in the minimum principal stress plot of figure 16. The mode transition of polarization displacement fields that was predicted at higher fiber-volume fractions was confirmed.

Potential applications are numerous. With this method, we are currently studying the interaction of waves with damage in laminated composites and the design of NDE arrays that match predicted wave topologies.

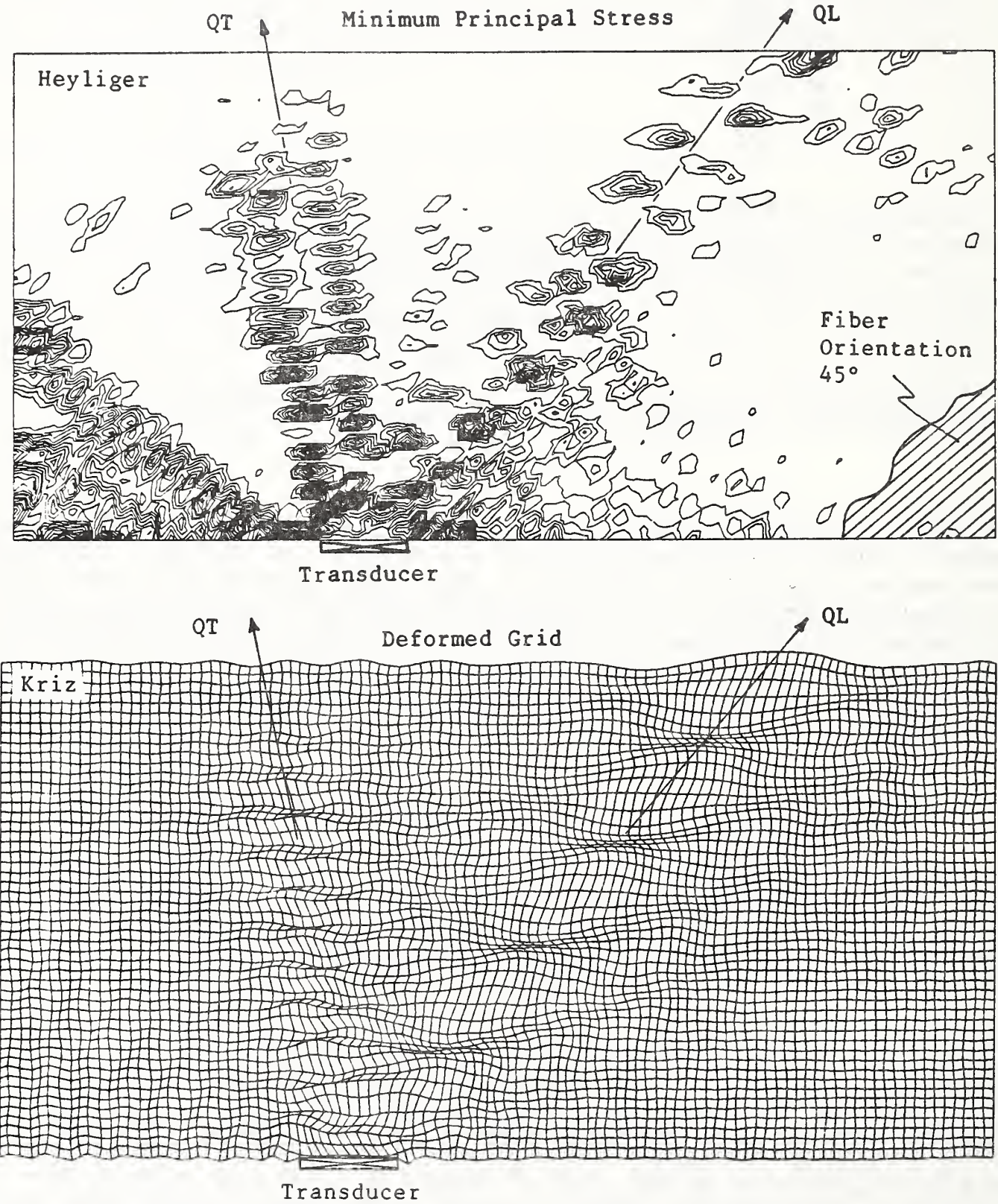


Figure 16. Stress-wave propagation in unidirectional graphite/epoxy, 45° off-axis.

### C. *Nondestructive tests of particle-reinforced rocket fuel*

Young's modulus and internal friction were measured for forty specimens of solid rocket fuel with a resonance NDE technique. Previous pulse-echo NDE techniques produced results with a wide scatter in localized areas. The resonance technique tests the entire volume of this particle-reinforced material, which decreases scatter of results. Because specimens were not cut to resonance length, Young's modulus was calculated from  $E_n = n^2E$ , where  $E$  is measured and  $n = 1, 2, 3, \dots$ . Future tests will relate the formation of microvoids to changes in internal friction measurements, which will lead to a better understanding of the natural aging process of these particle-reinforced composites. These microvoids initiate as interfacial debonding around imbedded particles.

### Reference

Moulder, J. C.; Read, D. T.; Cardenas-Garcia, J. F. (1986). A new video-optical method for whole-field strain measurements. *Proceedings, 1986 SEM Spring Conference on Experimental Mechanics*. Bethel, Connecticut: Society for Experimental Mechanics. 700-705.



## PROPERTIES

The Cryogenic Materials and Physical Properties Groups investigate the behavior of materials at low temperature and measure and model the physical properties of advanced materials, including composites, ceramics, and the new high-critical-temperature superconductors.

### Cryogenic Materials



Richard P. Reed  
Group Leader

L. M. Delgado, J. K. Han,\* T. Daniels, H. Lee,\* C. J. King,  
L. Ma,† P. T. Purtscher, N. J. Simon, R. L. Tobler, R. P. Walsh

We study the mechanical, physical, and metallurgical properties of materials in the temperature range 4 to 295 K. Goals of our research are the characterization and development of metals, alloys, and composites; the development of testing procedures and standards; and the collection and evaluation of material properties data.

A major program in recent years has been the development of materials technology to design and build superconducting magnets for fusion-energy systems. Because of our expertise in and unique facilities for measuring tensile, shear, creep, and fatigue properties, we provide testing services, design and safety assessments, and consultation on material selection and properties for a wide range of cryogenic projects.

### Representative accomplishments

- The interstitial strengthening of austenitic stainless steels was evaluated from room temperature to 4 K.

---

\*Guest worker from Korea Advanced Institute of Science and Technology, Seoul, Korea.

†Guest worker from the Institute of Metals, Shenyang, China.

- Selected mechanical and physical properties of indium were determined in the temperature range 4 to 295 K.
- Standards for tensile and fracture-toughness testing at 4 K were developed in a United States–Japan cooperative program and submitted to the American Society for Testing and Materials.
- The properties of copper and beryllium copper from over one thousand documents were added to our data base on cryogenic materials.

### Interstitial strengthening of austenitic steels

Structural alloys that can withstand the large magnetic forces of superconducting magnets are needed. Since structural failure in these applications would result in unacceptable loss, these alloys must also have excellent fracture toughness. Many of the low-temperature applications, such as those in magnetic-fusion-energy reactors and high-energy-physics magnets, require materials with high elastic moduli and low thermal and electrical conductivities. Austenitic steels have been selected almost exclusively for these uses. Recently, the Japan Atomic Energy Research Institute has urged the Japanese steel companies to develop even stronger and tougher austenitic steels (1200-MPa yield strength and  $200\text{-MPa}\cdot\text{m}^{1/2}$  fracture toughness at 4 K) for future use for structural constraint in large magnetic fields. Research in Japan to achieve these goals, coupled with research at NIST and other U.S. laboratories, has led to additions of nitrogen to achieve higher strengths at low temperatures for both Fe–Cr–Ni and Fe–Mn–Cr austenitic steels.

Additions of carbon and nitrogen to Fe–Cr–Ni-base austenites strongly increase the yield and other flow strengths at low temperatures [publication 48]. This is illustrated in figure 17 for temperatures of 4, 76, and 295 K. Despite its smaller atomic size, nitrogen increases the yield strength at 4 K more than carbon by a factor of 1.4. Both carbon and nitrogen contribute equally to the strength at 295 K. At 295 K, nitrogen also has a larger strain-misfit parameter than carbon. The modulus-misfit parameter of the carbon-plus-nitrogen content ( $[C+N]$ ) is negative at 295 K and positive at 4 K; this transition implies increased covalent bonding at low temperatures, primarily that of nitrogen. The strengthening increase at low temperatures from C+N addition ( $\sim G/2.5$ , where  $G$  is shear modulus) is of the same order as carbon in nickel at low temperatures.

The values of the strain-rate sensitivity parameter,  $m = \partial \ln \dot{\epsilon} / \partial \ln \sigma$ , were low. This implies that the stress field of the obstacle was short range. Correspondingly, the activation volumes,  $V^*$  were very low, especially at 4 K, where they were measured within the range 2 to  $5b^3$ , where  $b$  is Burgers vector. These low values imply very localized interaction volumes. When the case of a uniform array of obstacles is considered,  $V^*$  equals  $bld$ , where  $l$  is the average length of activated moving dislocation segments and  $d$  is the effective diameter of the obstacle. For 1 atomic percent [C] or [N], the average spacing of interstitial obstacles is about  $4b$ . The distance from the center of an octahedral hole in an fcc lattice to the

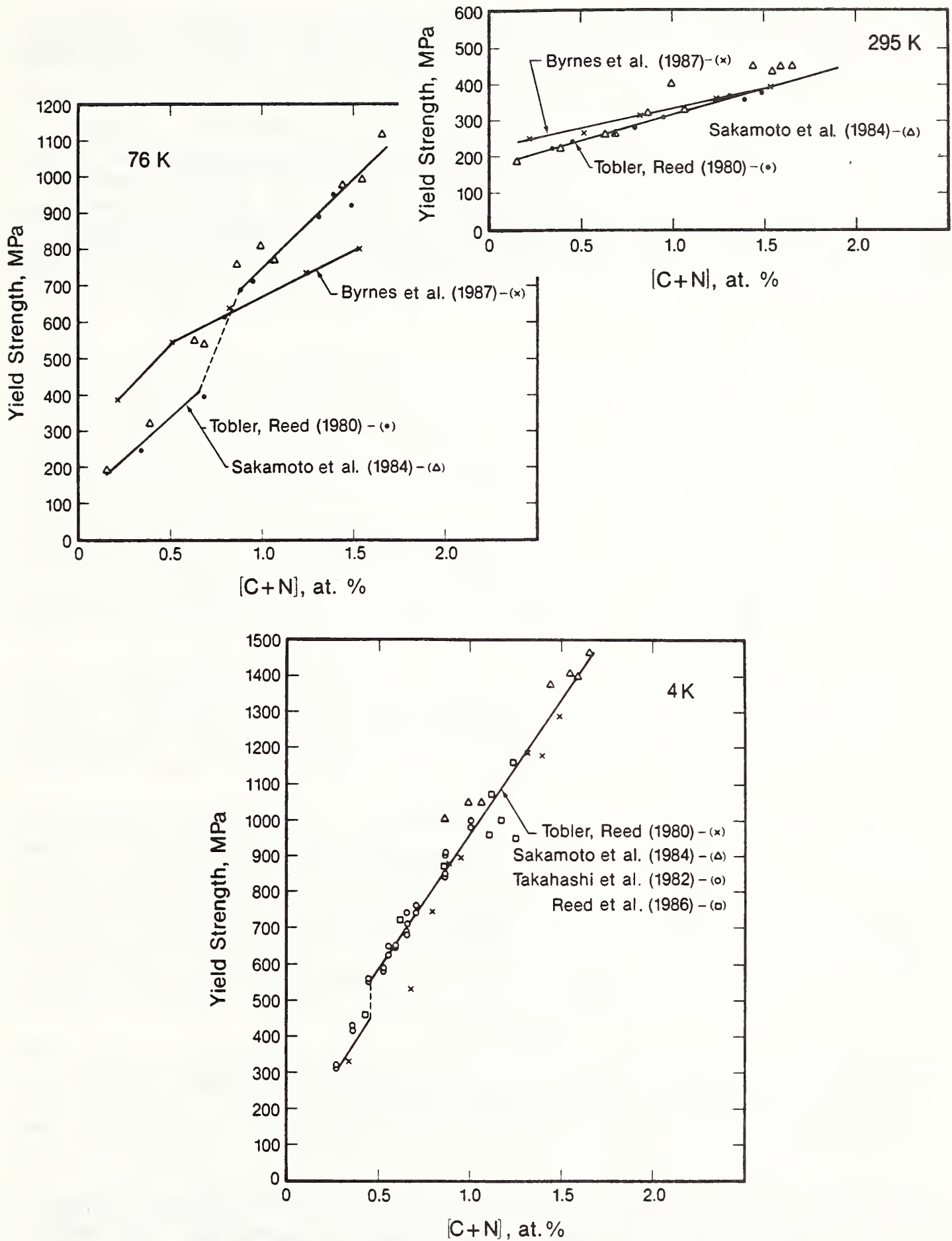


Figure 17. Low-temperature tensile-yield strengths for a series of austenitic stainless steels with varying [C+N].

nearest solvent atom is  $b \cdot 2^{1/2}$ . If we consider that this distance represents the effective interstitial diameter,  $b \ell d$  equals  $2^{3/2} b^3$ , which is very close to the 4-K values.

The observed dependence of  $V^*$  on [C+N] (fig. 18) is reasonable. Higher interstitial contents would effectively reduce  $\ell$ , creating more (and closer) activation sites. The ratio of the change of  $V^*$  from 0.5 atomic percent [C+N] to 1.5 atomic percent [C+N] was about 1.7 and was quite consistent at each temperature. The expected variation of uniformly spaced discrete obstacles of such concentrations is from  $\ell = 5.7b$  to  $3.5b$ , a ratio of 1.6—certainly very close for these estimates.

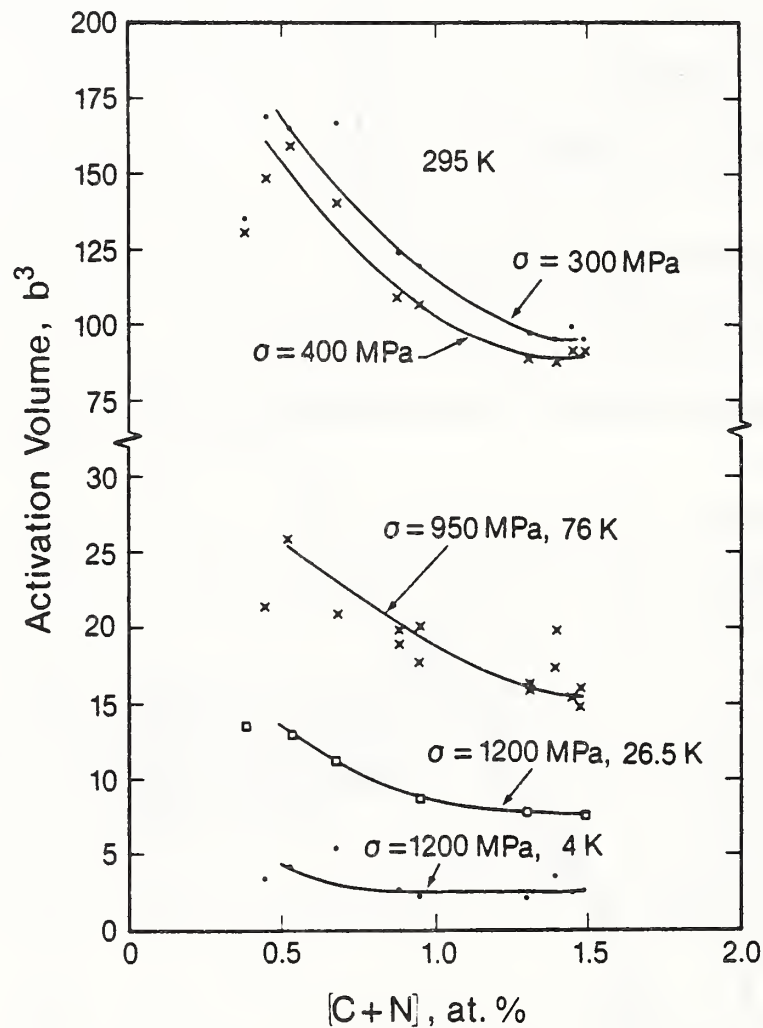


Figure 18. Operational activation volume ( $V^*$ ) versus [C+N] for selected true stress levels.

The dependence of operational activation volume,  $V^*$ , on temperature and individual strain-rate-change data is also shown in figure 18. The very low values of  $V^*$  imply strengthening from obstacles with strong, short-range stress fields. Also, the flow-strength temperature-dependence parameters suggest that Friedel statistics with a dominant strain

interaction best describe [C+N] strengthening in austenite at low temperatures. This description also fits best with the misfit parameters. The strain misfit of [C+N] is larger than that of solute elements and accounts, at least partially, for interstitial strengthening.

### Indium: Mechanical and Physical Properties

Indium and indium alloys are used extensively in high-technology applications because their excellent wetting characteristics enable reliable joining of glass, ceramics, or metals. Recent failures of indium solder joints in space applications have led to our research on its low temperature properties [publication 51].

Indium is the softest metal that is stable in air. During rolling or other forming operations at 295 K, indium softens as a result of deformation-induced recrystallization. The primary reason for the softness of indium at 295 K ( $T_r$ ) is the proximity of its melting temperature ( $T_m = 429$  K;  $T_r/T_m = 0.69$ ). Although the crystal structure of indium is commonly called face-centered tetragonal, its true space group is  $D_{4h}^{17}$  ( $I4/mmm$ ),  $A = 2$ ; thus, its structure is actually body-centered tetragonal. Nominal lattice constants are  $a = 0.32512$  nm,  $c = 0.49467$  nm,  $c/a = 1.5215$ . This tetragonality of structure ensures that its physical properties, such as thermal expansion and elastic constants, are anisotropic. Indium is diamagnetic and becomes superconducting at about 3.4 K.

Selected mechanical and physical properties of indium were determined in the temperature range 4 to 295 K. Tensile properties, creep, axial fatigue, torsion, and torsion fatigue were measured to assess mechanical performance. Elastic properties, thermal expansion, and electrical resistivity were measured to understand the low-temperature structure.

Twinning was prevalent as a deformation mode at all temperatures. Most tensile load-strain curves included some serrated yielding at all temperatures. We associate the serrations with deformation twinning. Even when metallography was used, care had to be taken to identify deformation twins. A pair of identical rectangular specimens was polished and then deformed in compression at 76 and 295 K. Figure 19 shows the combination of slip traces and deformation twins are shown following compressive deformation at 76 K. The twin traces are not the same as the slip traces.

Deformation twin planes had been identified as (10T) and 1T0); across other {110} planes, the twin symmetry already existed in the face-centered tetragonal lattice. The twins observed typically had one linear side and one curvilinear side. Presumably, the linear trace is stable and represents the compositional plane (10T) or 1T0). The curved interface had been mobile, providing twin growth. Most twins appeared to nucleate at grain boundaries. With one end originating from the grain boundary, twins terminated in the interior of the grain. The interior-grain-twin interface was lenticular on one side.



In figure 20, the stress at which serrations were first observed in the stress-strain curves is plotted vs. test temperature. The yield and ultimate strengths and the stress at which serrations ceased are also included. Usually, twinning-associated serrations began close to the yield strength and terminated slightly below the ultimate strength. However, there were large specimen-to-specimen variations in these stresses, as evidenced by the wide data bands. Stress averages reached maxima at temperatures between 10 and 76 K, but the data spreads were too large to place much credence in these maxima.

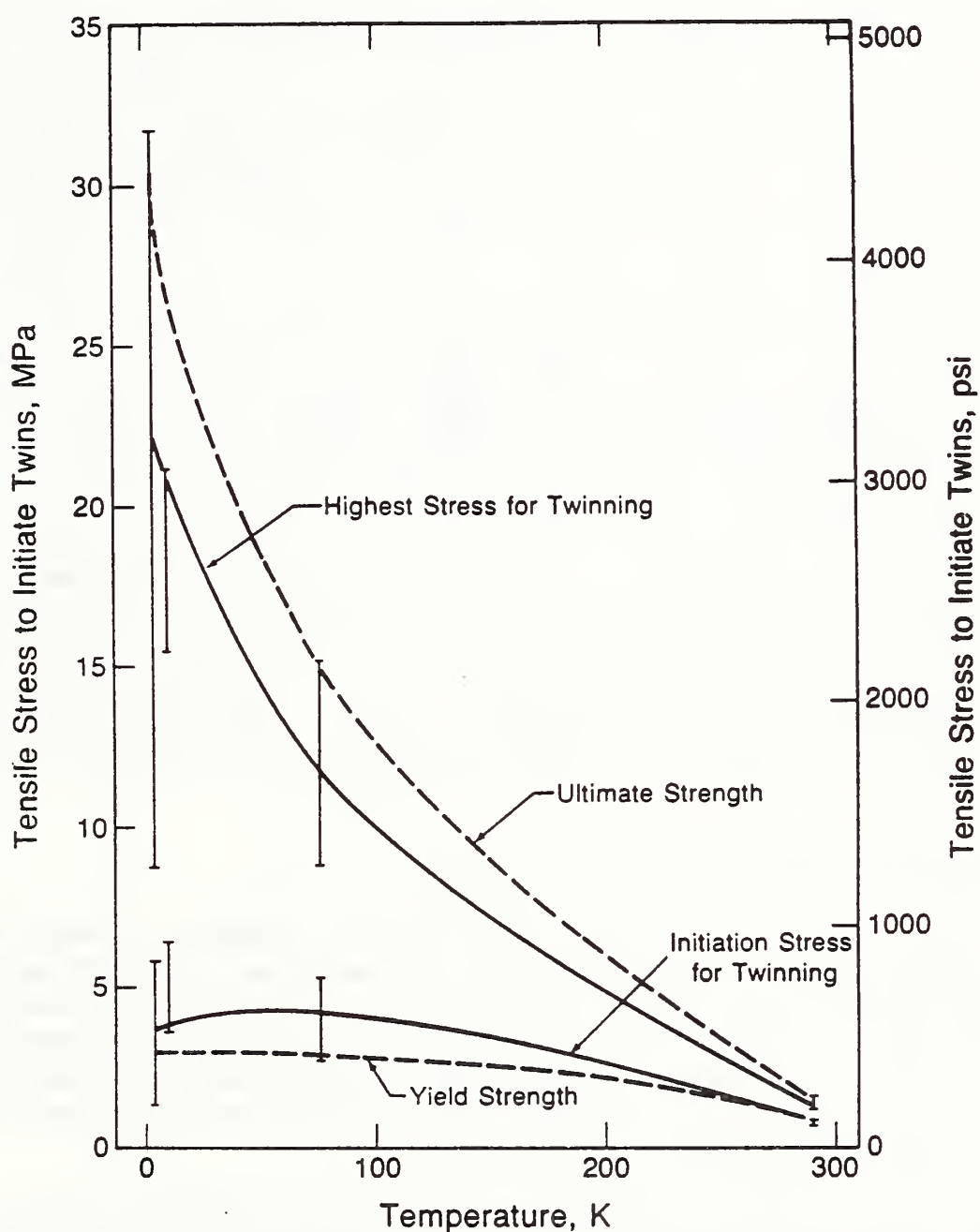


Figure 20. Stresses for onset and cessation of serrations in stress-strain curves; the serrations are associated with deformation twinning.

At room temperature, indium recrystallized during deformation; after low-temperature mechanical-property tests, indium recrystallized on warming to room temperature. At room temperature, indium failed in shear; at low temperatures, failure was usually by microvoid coalescence and dimpled rupture, followed by shear. In fatigue at low temperatures, microcracks were observed. The microcracks may be associated with grain boundaries or precipitates. In general, indium displayed characteristics similar to those of a soft face-centered metal.

#### United States-Japan program for the development of test standards

A United States-Japan cooperative program is developing tensile and fracture toughness testing standards for austenitic stainless steels (construction materials for superconducting machinery) at 4 K. Sponsors of the program are the U.S. Department of Energy, Office of Fusion Energy, and the Japan Atomic Energy Research Institute (JAERI). The program includes personnel exchanges, interlaboratory testing, and individual or cooperative research programs. Contributing organizations include NIST, three other American laboratories, JAERI, and six other Japanese laboratories.

During this program, which started in 1986, cryogenic materials scientists were interviewed at government, industrial, and academic institutions in Japan. Workshops were held in Sendai (March 1986 and January 1987), Reno (October 1986) and Tokai-mura (August 1986 and May 1988). The first and second round-robin tensile and fracture tests of Fe-13Cr-22Mn and Fe-25Cr-15Ni austenitic stainless steels were completed by June 1988 [publication 39]. The proposed standard 4-K tensile test procedure has been written and revised five times [publication 77]. Five drafts of the proposed 4-K fracture test standard were also prepared [publication 78]. In addition, an experimental matrix of eighty tests was executed at five laboratories to answer questions about test procedures. Six joint research papers were published [publications 39, 40, 41, 62, 75, 81]. The draft standards have now been submitted to ASTM for review and approval as consensus standards.

#### Material properties handbook

The Materials Handbook for Fusion Energy Systems (MHFES) is being developed to provide an authoritative common source of material properties for the fusion energy community to use in concept evaluation, design, safety analysis, and performance prediction and verification of fusion energy systems. This single source for properties is essential to ensure a common basis for material selection and design of the various fusion systems currently under study, in operation, or under construction.

We are continuing to work on handbook pages for the MHFES covering low-temperature properties of structural alloys for the superconducting magnets. Mechanical properties (including tensile properties, fracture toughness, fatigue and creep) and physical properties (including thermal,

electrical, and mechanical properties) are included in the temperature range from 0 to 300 K. Three nitrogen-strengthened austenitic stainless steels that are the most promising near-term candidates for structural use in superconducting magnets were chosen for initial coverage. Evaluation and analysis of copper (CDA 101-107) has been recently completed.

## References

Byrnes, M. L. G.; Grujicic, M.; Owen, W. S. (1987). *Acta Metall.* 35: 1853-1862.

Reed, R. P.; Purtscher, P. T.; Yushchenko, K. A. (1986). Nickel and nitrogen alloying effects on the strength and toughness of austenitic stainless steels at 4 K. Reed, R. P.; Clark, A. F., eds. *Advances in Cryogenic Engineering - Materials*, vol. 32. New York: Plenum. 43-50.

Sakamoto, T.; Nakagawa, Y.; Yamauchi, I.; Zaizen, T.; Nakajima, H.; Shimamoto, S. (1984). Nitrogen-containing 25Cr-13Ni stainless steel as a cryogenic structural material. Clark, A. F.; Reed, R. P. *Advances in Cryogenic Engineering - Materials*, vol. 30. New York: Plenum. 137-144.

Takahashi, Y.; Yoshida, K.; Shimada, M.; Tada, E.; Miura, R.; Shimamoto, S. (1982). Mechanical evaluation of nitrogen-strengthened stainless steels at 4 K. Reed, R. P.; Clark, A. F., eds. *Advances in Cryogenic Engineering - Materials*, vol. 28. New York: Plenum. 73-82.

Tobler, R. L.; Reed, R. P. (1980). *Materials Studies for Magnetic Fusion Energy Applications at Low Temperatures - III*. Nat. Bur. Stand. (U.S.) 15-48.

## Physical Properties



Hassel M. Ledbetter  
Research Leader

M. W. Austin, S. A. Kim, M. Lei,\* R. R. Rao†

Our research on deformation emphasizes measurements and modeling of elastic constants and related physical properties for metals, alloys, composites, ceramics, and the new oxide superconductors. For many studies, the temperatures range between 295 and 4 K. The elastic constants, which relate deformation to stress, sustain our interest because they relate to fundamental solid-state phenomena: interatomic potentials, equations of state, and phonon spectra. Furthermore, thermodynamics links elastic constants with specific heat, thermal expansivity, atomic volume, and the Debye temperature.

### Representative accomplishments

- The individual alloying effects on the elastic constants were determined for Fe-Cr-Ni-Mn austenitic steels.
- The five anisotropic elastic constants of graphite fibers were deduced by measuring the elastic constants of Gr/Al and Gr/Mg composites and using our theoretical model inversely.
- The complete set of elastic constants, from 5 to 295 K, of Y-Ba-Cu-O, Ho-Ba-Cu-O, and Eu-Ba-Cu-O were determined by ultrasonic methods.

---

\*Graduate student from the Institute of Metal Research, Shenyang, China.

†Guest worker from the Indian Institute of Technology, Madras, India.

## Austenitic steels

We determined the effects of several alloying elements—chromium, nickel, molybdenum—on the elastic constants of Fe-Cr-Ni alloys. All three increase the bulk modulus,  $B$ , and decrease the shear modulus,  $G$ . In most alloys, these two properties show parallel behavior. In these complicated 3d-electron transition-metal alloys, the nonparallel  $B$ - $G$  behavior may result from changing the  $d$ -electron- $s$ -electron balance. Probably, the  $d$ -electrons determine the shear modulus, which depends mainly on interatomic-bond angles, and both  $d$ -electrons and  $s$ -electrons determine the bulk modulus, which depends only on interatomic-bond lengths. Applying a modified Ducastelle model to our measurements showed the relative contributions of repulsive energy and band-structure energy to the elastic constants. For both 4 and 295 K, figure 21 shows the fractional band-structure-energy contribution to the bulk modulus. We see a lower contribution at low temperatures and a decrease with the addition of carbon and nitrogen, which increase the unit-cell volume.

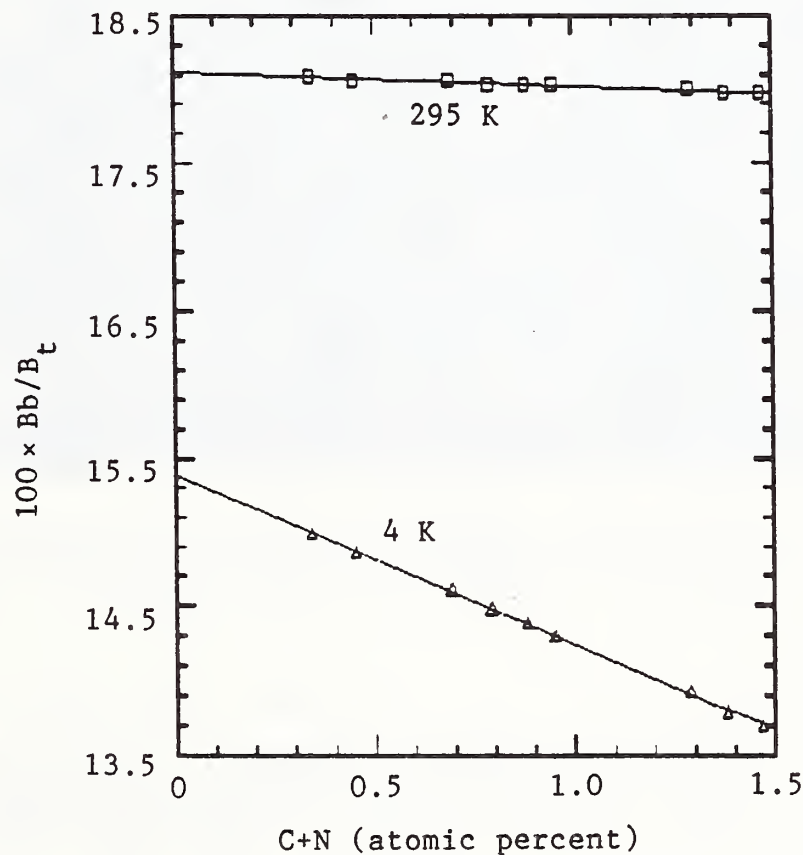


Figure 21. Percentage contribution of band-structure energy to total bulk modulus. Effect of alloying interstitial carbon and nitrogen into Fe-Cr-Ni alloy.

## Composites

We determined the complete five-component transverse-isotropic-symmetry elastic-constant tensor for two graphite fibers: one with high strength and low modulus and one with low strength and high modulus. We did this in two steps. First, we measured ultrasonically the complete elastic constants of a metal matrix with embedded uniaxial graphite fibers [publication 10]. Second, we did an inverse-modeling calculation to extract the fiber's elastic constants. This calculation requires three inputs: composite elastic constants, matrix elastic constants, and fiber-matrix phase geometry, principally the fiber volume fraction. We compared the results with those expected for a random quasi-isotropic graphite aggregate and for a hypothetical graphite fiber with perfectly aligned basal planes. Figure 22 shows the composite's microstructure.

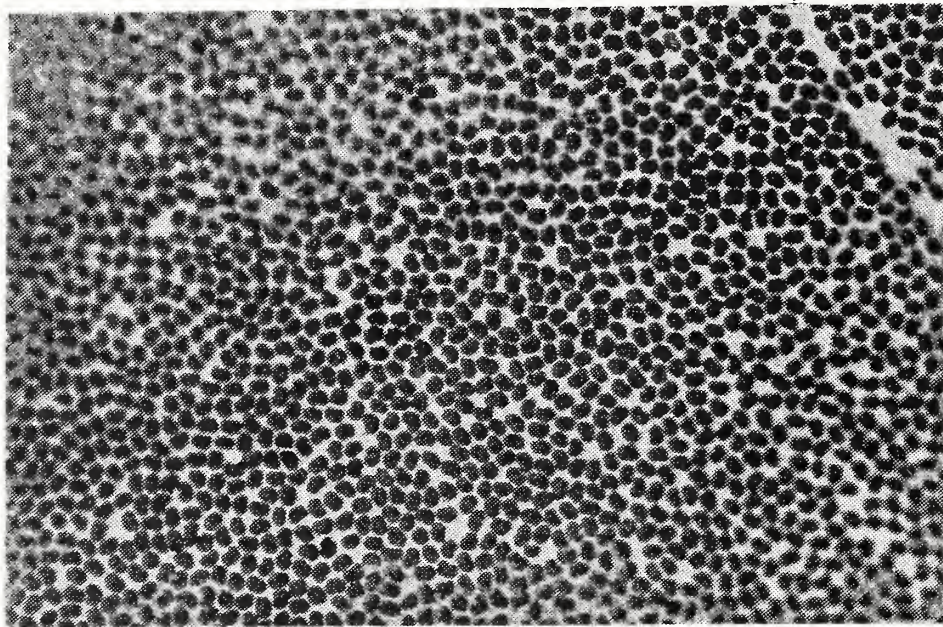


Figure 22. Optical photomicrograph of transverse section of graphite-fiber-reinforced magnesium-matrix composite. The fibers, 7  $\mu\text{m}$  in diameter, occupy 70 volume percent of the composite.

Graphite possesses remarkable physical properties. For example, the within-basal-plane Young's modulus equals 902 GPa, four times that of iron (212 GPa), and 80 percent of that of diamond (1141 GPa). Also, graphite exhibits strong physical-property anisotropy: the  $E_1/E_3$  Young's-modulus ratio equals 29.8. (Here, subscript 1 denotes any direction in the basal plane, which is isotropic, and subscript 3 denotes the axis perpendicular to the basal plane.)

The fiber's elastic constants provide a valuable material characterization: information on basal-plane alignment. Also, they enter many practical problems, such as internal strain (residual stress).

## Superconductors

Using ultrasonic methods, we determined the complete set of elastic constants, from 5 to 295 K, of several high- $T_C$  metal-oxide superconductors: Y-Ba-Cu-O, Ho-Ba-Cu-O, Eu-Ba-Cu-O [publications 23-25, 29-31]. Focusing on the yttrium oxide, we studied six specimens prepared at four laboratories. The bulk modulus, corrected to the void-free state, ranged from 54 to 101 GPa. Poisson's ratio,  $0.21 \pm 0.02$ , compares closely with that of  $\text{BaTiO}_3$  (0.223) and  $\text{SrTiO}_3$  (0.236), suggesting similar interatomic bonding. At  $T_C$  (near 91 K), within measurement error (0.1 percent), the elastic constants showed no discontinuity.

To compare various physical-property measurements, we focused on the Debye temperature,  $\theta$  [publication 25]. For example, from the elastic constants of Y-Ba-Cu-O, we found  $\theta = 423$  K; from specific heat,  $\theta = 440$  K; from thermal expansion,  $\theta = 370$  K; from hardness,  $\theta = 677$  K. This wide range in  $\theta$  is inconsistent with fundamental interrelationships among related physical properties.

We studied ultrasonic-wave velocities, both longitudinal and shear, in  $\text{Y}_1\text{Ba}_2\text{Cu}_3\text{O}_{7-x}$  between 5 and 295 K during both cooling and warming [publication 11]. Both waves, especially the longitudinal, showed thermal hysteresis. The results suggest a hysteretic phase change that occurs between 160 and 70 K during cooling and between 170 and 260 K during warming. This phase-change hypothesis explains anomalies in several physical properties. The phase change agrees with predictions of thermodynamic instability. We confirmed the hysteresis in Ho-Ba-Cu-O, where it is smaller than in Y-Ba-Cu-O, and in Eu-Ba-Cu-O, where it is larger. In a companion perovskite,  $\text{BaTiO}_3$ , we observed zero hysteresis. At  $T_C$ , 91 K, sound velocities showed no measurable change in either magnitude or slope. This continuity disputes the current popular view that, contrary to thermodynamics, elastic stiffness increases upon cooling through  $T_C$  into the superconducting state. We believe that stiffening results from the usual thermal effects after a phase transformation from a stiffer phase. Figure 23 shows the hysteresis in three elastic constants:  $G$ , shear modulus;  $B$ , bulk modulus, and  $\nu$ , Poisson's ratio.

We studied the elastic constants from 4 to 295 K of another type of superconductor: the Chevrel-phase  $\text{PbMo}_6\text{S}_8$ . The elastic constants show strong temperature anomalies and strong associated anomalies in attenuation. Cooling to 4 K brings about significant internal changes not attributable to a crystal-structure change.

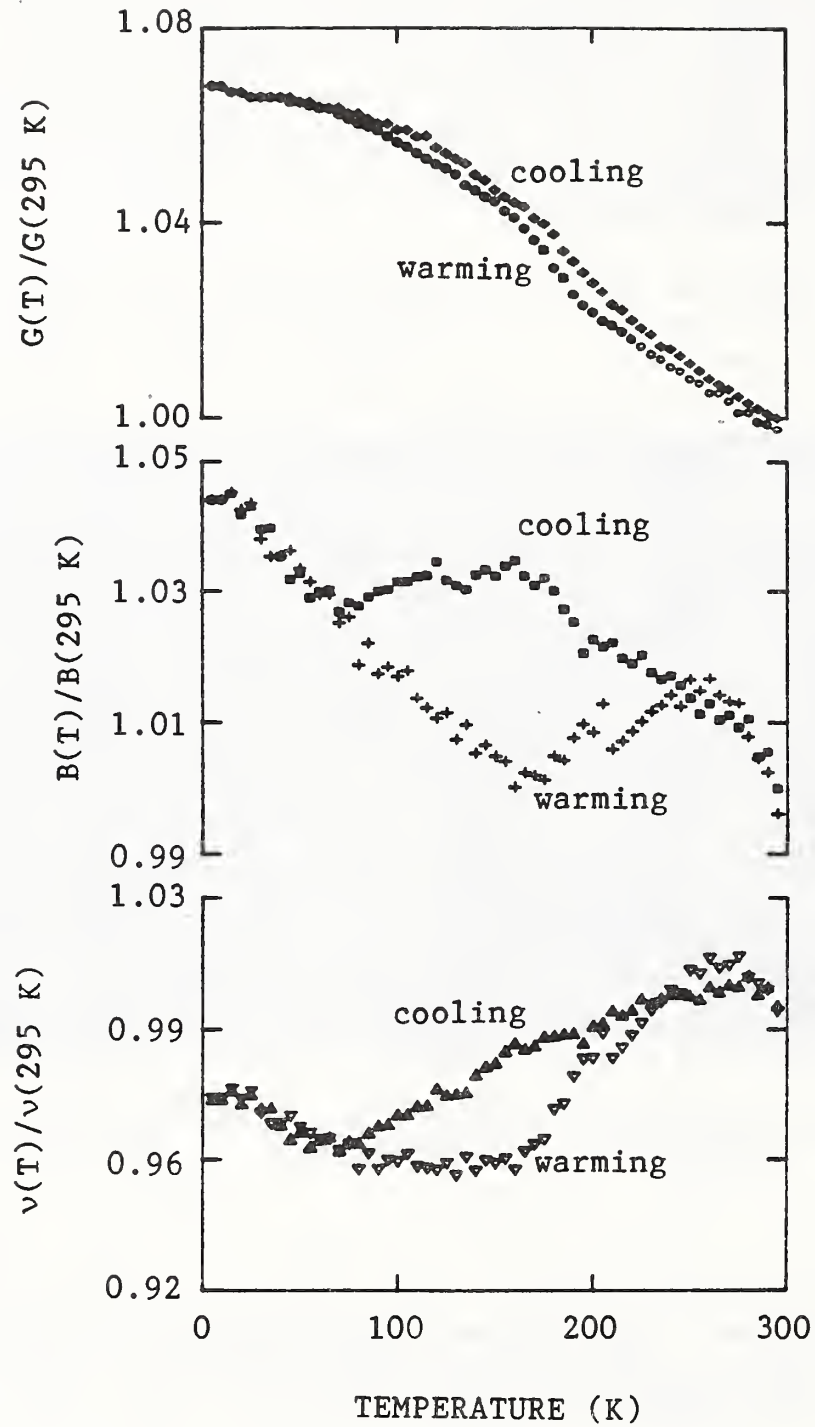


Figure 23. For  $Y_1Ba_2Cu_3O_{7-x}$ , temperature variation of shear modulus,  $G$ ; bulk modulus,  $B$ ; and Poisson's ratio,  $\nu$ . Note the large thermal hysteresis, especially in longitudinal modes.

## Studies related to nondestructive evaluation

Although our sound-velocity studies, experimental and theoretical, proceed mainly toward determining solid-state physical properties, many studies relate to nondestructive evaluation.

Our study of a composite with continuous, uniaxial graphite fibers (70 volume percent) in a magnesium matrix included measurement, modeling, and inverse modeling to obtain the fiber's elastic constants. By ultrasonic-velocity methods, we measured the composite's complete orthotropic-symmetry elastic-constant tensor— $C_{ij}$  in Voigt contracted notation. Approximately, the composite shows transverse-isotropic symmetry. For a model, we used a wave-scattering method in the long-wavelength limit. The model requires two inputs: the two isotropic matrix elastic constants and the five anisotropic fiber elastic constants. We measured the first and guessed the second on the basis of graphite-fiber elastic constants reported by others. This guess gave good measurement-model agreement for only  $C_{11}$ ,  $C_{22}$ , and  $C_{33}$ . Especially, the shear moduli  $C_{11}$  ( $i = 4, 5, 6$ ) agreed poorly (a 20-percent difference). Using inverse modeling (calculation of fiber properties from measured matrix properties and measured composite properties), we estimated the anisotropic fiber elastic constants. For the fiber, we predict a Young's modulus anisotropy of 12 and a principal range of Poisson's ratio from 0.03 to 0.37. We also showed the neutron-diffraction textures for both the matrix and the fiber.

Using a scattered-plane-wave ensemble-average model developed for composite materials, we calculated the effective elastic constants of cast iron. We focused on the effect of graphite-particle aspect ratio on Young's modulus. Between model and observation, we found good agreement. Oblate-spheroidal graphite flakes lower the elastic stiffnesses much more than do spheres. To obtain good model-measurement agreement, we must use graphite's lower third-order-bound (Kröner-bound) elastic constants. Besides Young's modulus, we calculated the usual quasi-isotropic elastic constants: shear modulus, Poisson's ratio, and bulk modulus.

## Other studies

This year, other physical-property studies included the following materials: amber, barium titanate, strontium titanate, glass-epoxy composites, an alumina-fiber/(poly)ether-ether-ketone composite, and a silicon-carbide-particle/aluminum-matrix composite.

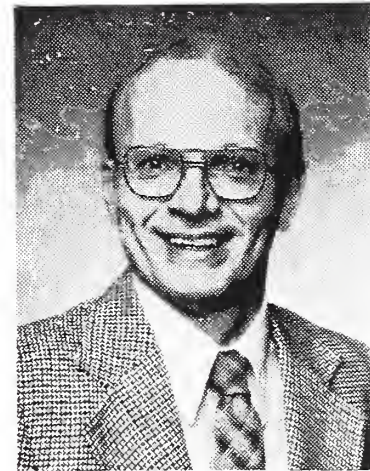
On the analytical-theoretical side, we focused on the thermoelastic coefficient and its pressure derivative. Using a Mie-Grüneisen interatomic potential, we derived a relationship for the thermoelastic coefficient  $K = -(1/T)(\partial T/\partial \sigma)$ , the temperature change caused by stress, and for the thermoelastic-coefficient pressure derivative,  $(1/K)(\partial K/\partial P)$ . The latter, related to third-order and fourth-order elastic constants, relates simply and approximately to the bulk-modulus temperature derivative,  $(1/B)(\partial B/\partial T)$ . Comparison with a solid-mechanics model shows agreement within approximately twenty percent.



## PROCESSING

The Welding and Thermomechanical Processing Groups investigate the non-equilibrium metallurgical changes that occur during processing, such as solidification, recrystallization, phase transformation, and precipitation strengthening. These changes affect the quality, microstructure, properties, and performance of metals.

### Welding



Thomas A. Siewert  
Group Leader

G. Adam,\* C. N. McCowan, D. A. Shepherd, D. P. Vigliotti

Since structural failures often originate at flaws in welds, the study of welding is integral to our structural safety research. Our goals are to develop procedures that reduce the incidence of defects and to develop weld metals with improved tolerance for defects. We use a computerized fully adaptive gas-metal arc-welding system to produce weld flaws for evaluation of nondestructive test methods and for the study of microstructure-toughness relationships in both the weld and heat-affected zone. Now we are using these same capabilities to develop automated process controls.

### Representative accomplishments

- A database of 950 welds was used to develop an improved diagram for predicting the ferrite content of stainless steel welds as a function of chemical composition.
- A prototype radiation-transfer standard has been developed for use as an image-quality indicator for real-time radiology.
- A gas-shielded arc-welding procedure has been developed to produce standard reference materials with uniform gas contents for use in calibrating residual gas analyzers.

---

\*Guest worker from the Nuclear Research Centre - Negev, Beer-Sheva, Israel.

## Stainless steel

In a cooperative program with the Welding Research Council, a diagram was developed that predicts the ferrite content of stainless steel welds with more accuracy than previous prediction diagrams [publication 72]. The new diagram shown in figure 24 was developed from a database of 950 welds, and it extends predictability to 100 FN (ferrite number). Certain ferrite ranges have been associated with cracking; others have been related to poor corrosion resistance. The improved accuracy of this diagram gives greater assurance that a composition will have the desired ferrite content. The diagram has been evaluated for accuracy as a function of alloy content using the 950-weld database from which it was developed. It has proven accurate within 2 FN for manganese contents to 10 mass percent, Mo contents to 3 mass percent, and nitrogen contents to 0.20 mass percent.

The Welding Research Council's Subcommittee on the Welding of Stainless Steel and the International Institute of Welding are evaluating the diagram with independent data. Upon successful completion of this evaluation, it will be submitted as a new standard to the American Welding Society and the American Society of Mechanical Engineers.

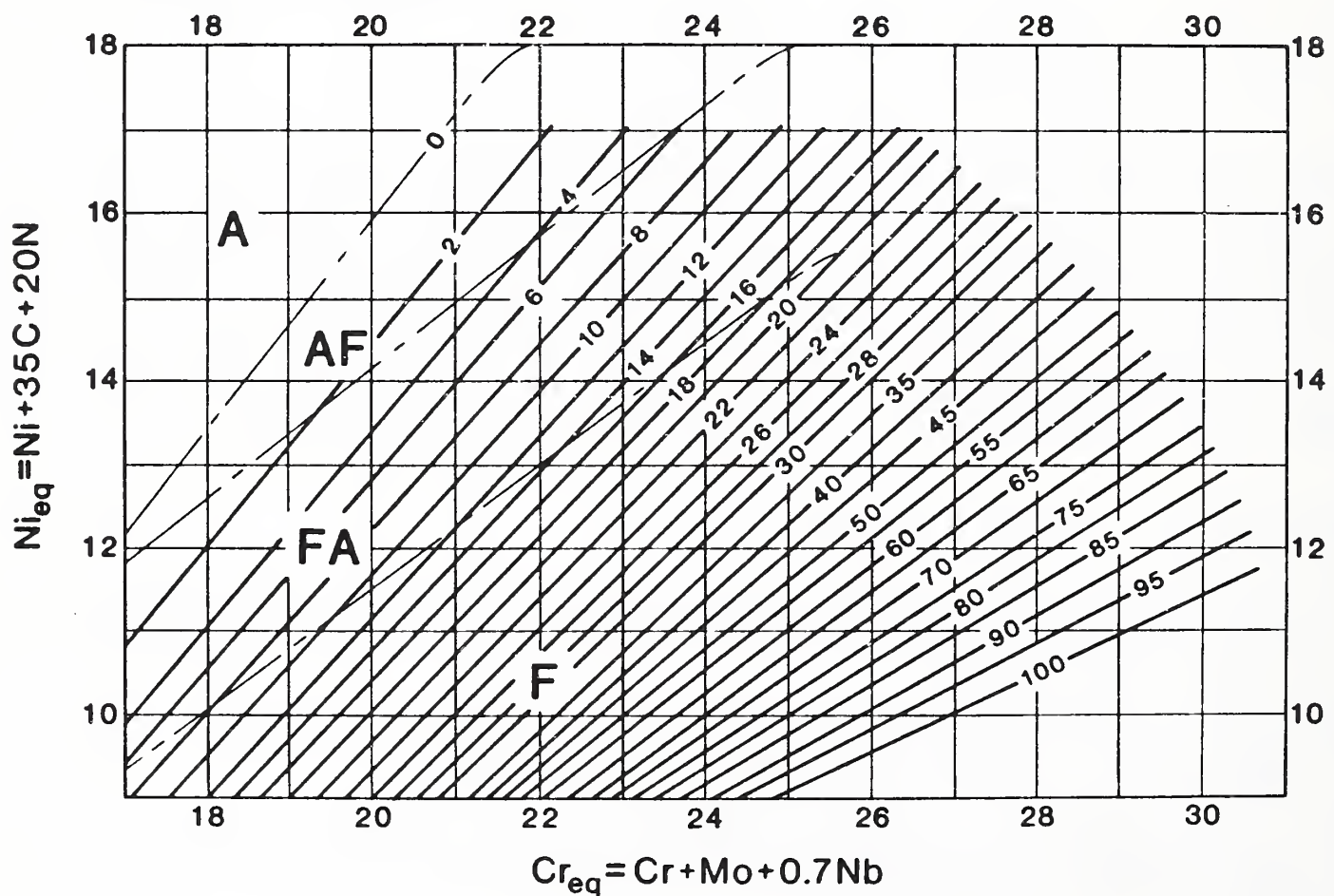


Figure 24. New ferrite-prediction diagram for stainless steel welds.

## Real-Time Radiology

Responding to the needs identified in the 1987 Workshop on Standards for Real-Time Radioscopy, we developed a questionnaire on real-time systems and their usage in this country. After a presentation at the 1988 ASTM winter committee meetings, committee members offered to complete the questionnaire. Preliminary results were reported at the 1988 summer committee meeting and at a topical conference of the American Society for Nondestructive Testing (ASNT) [publication 67]. The final report will guide the development of a radiation transfer standard in fiscal year 1989.

Current image-quality indicators, which were designed for film radiography must be repositioned for each exposure. Thus, with these indicators, we cannot exploit the advantages of real-time systems: dynamic evaluation and rotation of the specimen without repositioning the detection system. New standards are being developed to evaluate systems in real time. Prototype standards with one- and two-dimensional symmetry have been produced and are being evaluated; their design concept is illustrated in figure 25.

Cross Section

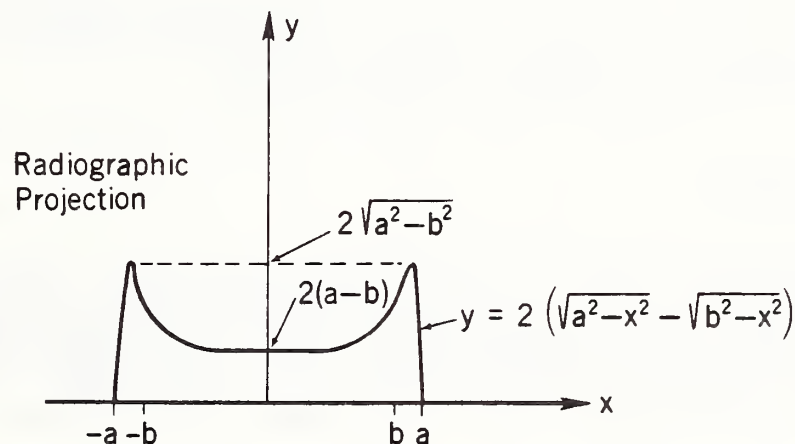
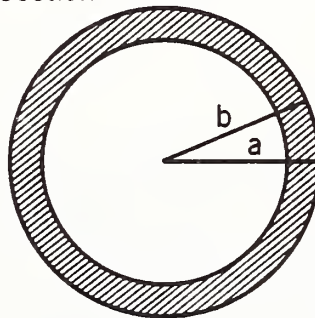


Figure 25. Real-time spheres.

## Arc Physics

The arc-physics equipment in our welding laboratory continues to generate cooperative programs. This spring, a graduate student helped to evaluate voltage changes as a means of characterizing droplet transfer in gas-metal arc welding [publication 34]. He found that voltage changes greater than approximately 8 V correlated with short-circuiting transfer and voltage changes between 1 and 4 V were associated with globular transfer. Intermediate voltage changes were associated with transitions between these modes, and voltage changes of less than 1 V were associated with spray transfer and electrical noise. These values are consistent with published data and models for voltage drops across the arc. The results provide another sensing methodology for intelligent closed-loop control of welding processes.

With the help of a guest worker, the data collection and processing capability is being upgraded. A digital oscilloscope with a 8-kilobyte memory is being replaced by a 16-MHz microcomputer with 1-megabyte RAM and a 100-kHz A-to-D board. Its larger memory and improved processing capability increase the resolution of transient behavior and the measurement of droplet transfer rate. We shall use the new system to study an HY-80 gas-metal-arc electrode; results will be compared with those of previous studies of a C-Mn electrode.

## Gases in metals

The dissolution of shielding gases into the weld pool, which is usually considered a disadvantage in welding, is being turned into an advantage: This technique is being used to develop standards for residual gas analyzers with uniform gas levels, levels above those attainable by casting techniques. To reduce specimen machining and variable penetration problems, the welds are made in a grooved copper block. Since the weld metal does not wet the copper, the cylindrical weld bead can be removed. Preliminary evaluation of nitrogen and oxygen in a C-Mn steel has demonstrated the feasibility of using the technique to produce standard reference materials. We are currently evaluating specimens of hydrogen in titanium.

## Analyses of fluxes

For many welding processes, the flux is an integral part of the electrode, and it is evaluated during qualification testing. Submerged arc welding is an exception; the electrode and flux come from independent lots. Thus, a flux-electrode combination could be chosen that would not meet the mechanical property requirements even though each had been qualified separately.

In support of standards development, we are evaluating techniques for analyzing welding fluxes. Our goal is to identify a method whereby we can control the flux composition and possibly predict other welding problems.

## Thermomechanical Processing



Yi Wen Cheng  
Research Leader

H. I. McHenry, D. A. Shepherd, Y. Rosenthal\*

Research in thermomechanical processing uses a deformation-processing simulator built at NIST. We study the metallurgical changes that occur in steels during controlled rolling and accelerated cooling. By controlling the temperature-deformation schedules, the cooling after rolling, and the subsequent tempering treatment, we are striving to achieve optimum strength and toughness in high-strength steels.

### Representative Accomplishments

- The NIST thermomechanical processing (TMP) simulator was used to study the recrystallization behavior and transformation kinetics of a precipitation-strengthened steel.
- A dilatometer that can resolve axial displacements of  $1 \mu\text{m}$  was developed to detect phase changes during accelerated cooling immediately after deformation processing.

### Thermomechanical processing simulator

A thermomechanical processing simulator has been designed and installed [publication 3]. The simulator has the following features:

- a servohydraulic load frame with a 250-kN capacity in tension or compression
- a dilatometer with a resolution of  $1 \mu\text{m}$
- an actuator with a variable traveling speed up to  $500 \text{ mm}\cdot\text{s}^{-1}$
- a multiple-strike capability with control-label displacements and strain rates

---

\*Guest worker from the Nuclear Research Centre - Negev, Beer-Sheva, Israel.

- a 10-kW induction heater with a maximum heating rate of  $150^{\circ}\text{C}\cdot\text{s}^{-1}$   
(for a cylindrical steel specimen 9 mm in diameter and 18 mm in height)
- helium-gas cooling with a maximum cooling rate of  $25^{\circ}\text{C}\cdot\text{s}^{-1}$
- vacuum to  $1.33 \times 10^{-3}$  Pa ( $1 \times 10^{-5}$  torr) within 25 min.

It can be used to study austenite recrystallization during hot deformation, hot-deformation resistance during single or multiple-strike deformation, and austenite phase transformation in terms of continuous-cooling transformation (CCT) and time-temperature-transformation diagrams. The austenite phase transformation is detected with a dilatometer that was designed to monitor phase changes immediately after hot working (the hot working simulates plate rolling or forging). Figure 26 shows temperature versus dilation for a sample of ASTM A710 steel. The dilatometer enables us to construct CCT diagrams from deformed austenite rather than the commonly used undeformed austenite.

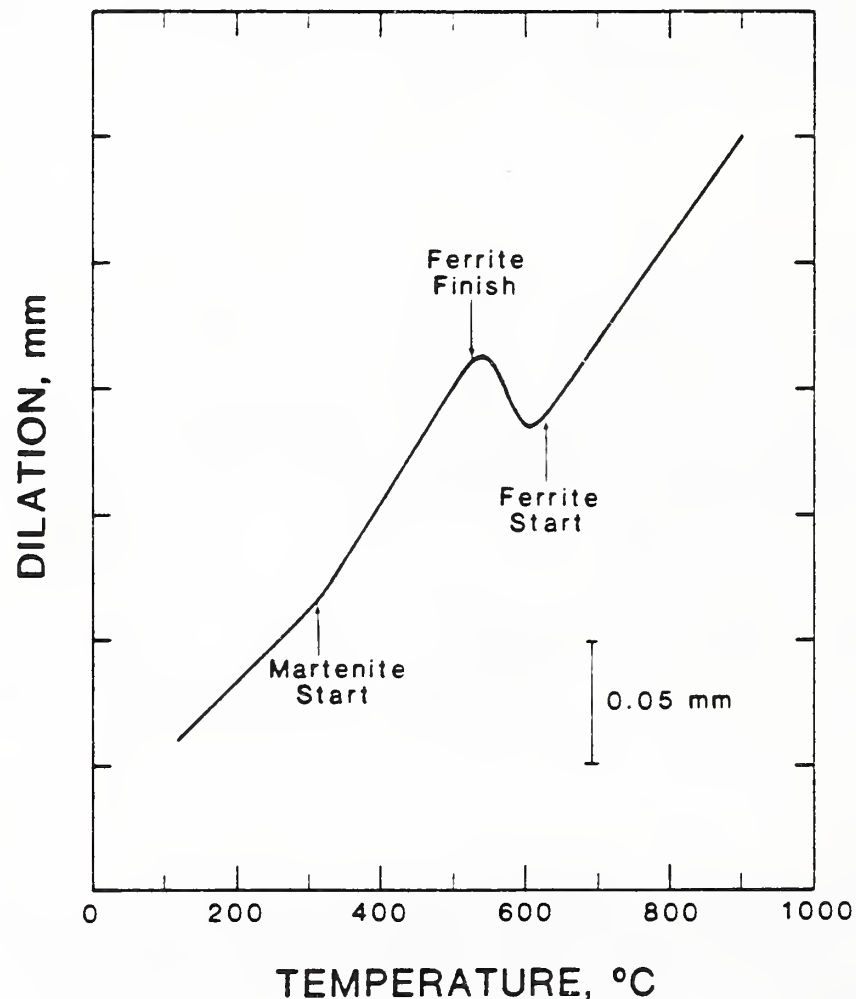


Figure 26. Dilatation curve for ASTM A710 steel.  $\Delta t(800/500^{\circ}\text{C}) = 22.5$  s.

## Phase-transformation studies

A study has been made of simulated controlled rolling followed by direct quenching (CR/DQ) of ASTM A710 steel. Experimental results indicated that the hardenability (bainitic) of the steel was greater after CR/DQ processing than after the conventional re-austenitizing and quenching treatment (fig. 27).

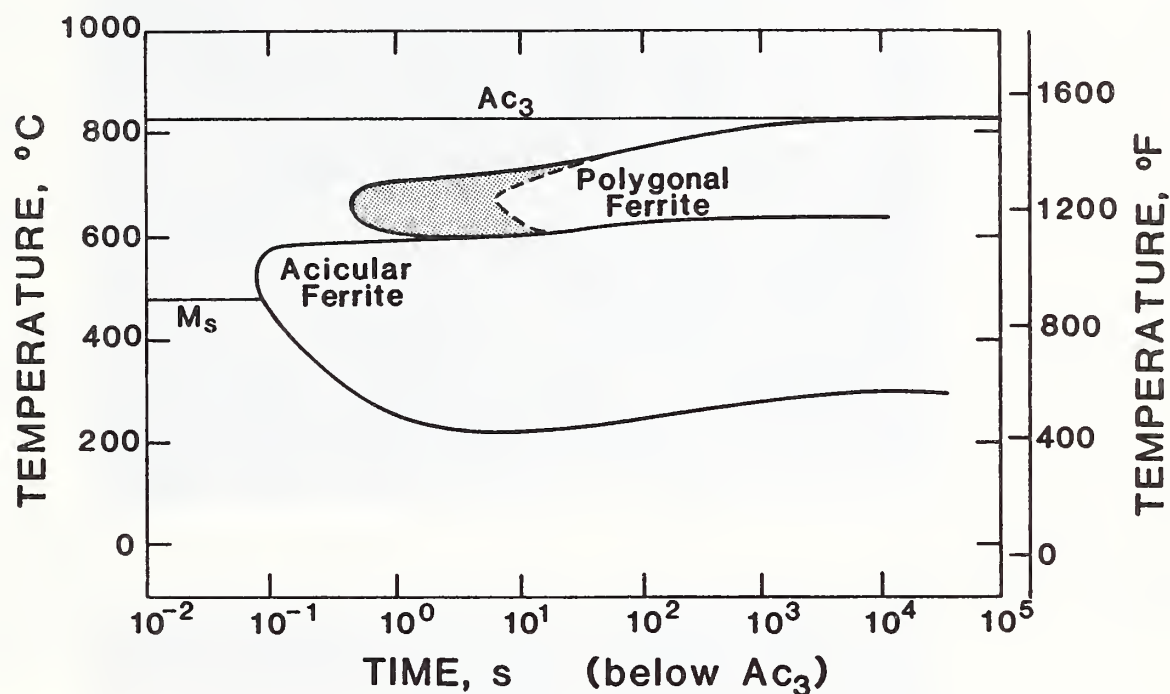


Figure 27. Simplified CCT diagram. The hardenability (bainitic) of ASTM A710 steel is increased with CR/DQ processing by an extent shown by the shaded area. The formation of polygonal ferrite is delayed about 10 s with CR/DQ processing; thus, acicular ferrite is easier to form. The advantage of acicular ferrite is that it is about 15 percent stronger than polygonal ferrite and nearly as tough.

With a cooling rate of about  $10^{\circ}\text{C}\cdot\text{s}^{-1}$ , the sample with re-austenitizing ( $910^{\circ}\text{C}$ ) and quenching treatment produced a predominantly polygonal ferrite microstructure, the white area in Fig. 28a. The dark areas in figure 28a are a mixture of pearlite, bainite, and martensite. With a similar cooling rate, the processing produced the acicular ferritic microstructure shown in figure 28b. The second-phase particles dispersed in figure 28b are a mixture of retained austenite and martensite. Acicular ferrite is also called granular bainite, which is different from classical bainite because it does not contain the second-phase cementite particles.

The increase in hardenability is attributed to the larger austenite grain sizes in CR/DQ-processed steel and to the dissolution of alloying elements in the austenite. The positive implication of the observation is that the strength of the steel can be increased with CR/DQ processing or the amounts of alloying elements can be reduced while maintaining the same strength level.

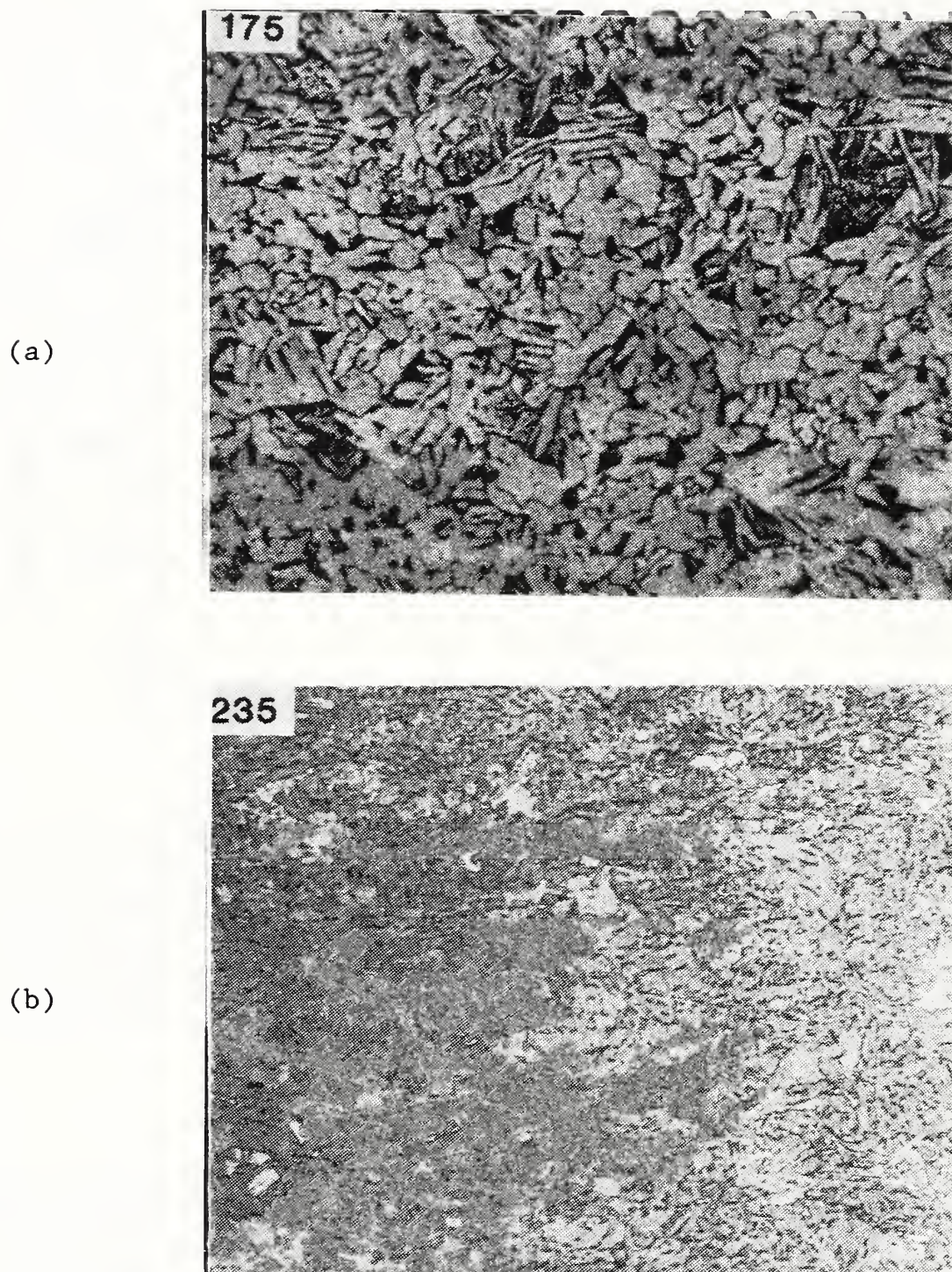


Figure 28. Microstructures formed at a cooling rate of about  $15^{\circ}\text{C}\cdot\text{s}^{-1}$  in ASTM A710 steel. (a) conventional re-austenitized at  $910^{\circ}\text{C}$  and quenched; polygonal ferrite dominated. (b) CR/DQ processed; acicular ferrite dominated.

## In-line accelerated cooling of steel plate

An advanced method of thermomechanically processing steel plates is to finish rolling them below their recrystallization temperature and cool them immediately. This continuous process of controlled rolling and accelerated cooling produces steel plates with properties in the as-rolled condition that equal or exceed those of heat-treated plates. The steel companies in Japan that have developed this technology have used it to produce millions of tons of steel plate. At the present time, the U.S. steel industry does not have the capability for in-line accelerated cooling.

To generate a domestic capability for in-line accelerated cooling, we assisted the Department of Defense in developing a Defense Production Act Title III Program entitled "Accelerated Cooling Processing of DOD Steels." Three American steel-plate producers are expected to participate in Phase I of the program, which has been funded in the fiscal year 1989 budget. The approach is to provide incentives for the American companies to purchase the technology and equipment from foreign companies.

This year our contribution to the Title III Program consisted mainly of liaison activities. We visited officials at the Ministry of International Trade and Industry and five Japanese steel companies; they agreed to cooperate in transferring the in-line accelerated cooling technology.

From three Japanese manufacturers, we obtained sample plates that were produced by advanced thermomechanical processing for evaluation in the United States. Their yield strengths were 450, 550, 700, and 900 MPa. Their mechanical properties typically met specified requirements despite significantly lower alloy contents.



OUTPUTS  
and  
INTERACTIONS



## SELECTED RECENT PUBLICATIONS\*

1. Auld, B. A.; Moulder, J. C.; Jefferies, S.; Shull, P. J.; Ayter, S.; Kenney, J. Eddy current reflection probes: theory and experiment. Submitted to *J. Res. Nondestruct. Eval.*
2. Berge, S.; Ebrahimi, F.; Read, D. T. Wide plates in bending: application of CTOD design approach. Read, D. T.; Reed, R. P., eds. *Fracture Mechanics: Eighteenth Symposium*. ASTM STP 945. Philadelphia: Amer. Soc. Test. Mater.; 1988. 516-534.
3. Cheng, Y.-W.; McHenry, H. I. A hot-deformation apparatus for thermo-mechanical processing simulation. Accepted for publication in *Proceedings of the International Symposium on Physical Simulation of Welding, Hot Forming, and Continuous Casting*.
4. Cheng, Y.-W. Fatigue crack growth analysis under seawave loading. *Int. J. Fatigue* 10(2): 101-108; 1988.
5. Clark, A. F.; Reed, R. P., eds. *Advances in Cryogenic Engineering - Materials*, vol. 34. New York: Plenum; 1988. 1072 pp.
6. Clark, A. V. Ultrasonic characterization of texture and formability. *Mater. Res. Soc. Bull.* XIII(4): 40-43; 1988.
7. Clark, A. V.; Blessing, G. V.; Thompson, R. B.; Smith, J. F. Ultrasonic methods of texture and monitoring for characterization of formability of rolled aluminum sheet. Thompson, D. O.; Chimenti, D. E. *Review of Progress in Quantitative Nondestructive Evaluation*, vol. 7B. New York: Plenum; 1988. 1365-1373.
8. Clark, A. V.; Reno, R. C.; Thompson, R. B.; Smith, J.; Blessing, G. V.; Fields, R. J.; Delsanto, P. P.; Mignogna, R. B. Texture monitoring in aluminum alloys: A comparison of ultrasonic and neutron diffraction measurement. *Ultrasonics* 26(4): 189-197; 1988.
9. Clark, A. V.; Schramm, R. E.; Fukuoka, H.; Mitraković, D. V. Ultrasonic characterization of residual stress and flaws in cast railroad wheels. McAvoy, B., ed. *Proceedings: IEEE 1987 Ultrasonics Symposium*. New York: IEEE; 1988. 1079-1082.
10. Datta, S. K.; Ledbetter, H. M.; Shindo, Y.; Shah, A. H.; Phase velocity and attenuation of plane elastic waves in a particle-reinforced composite medium. *Wave Motion* 10: 171-182; 1988.
11. Datta, T.; Ledbetter, H. M.; Violet, C. E.; Almasan, C.; Estrada, J. Reentrant softening in perovskite-like superconductors. *Phys. Rev. B* 37: 7502-7505; 1988.

---

\*Papers that were published or accepted for publication by the Editorial Review Boards of the National Institute for Standards and Technology during fiscal year 1988.

12. Denys, R; McHenry, H. I. Local brittle zones in steel weldments: an assessment of test methods. *Proceedings, Seventh International Conference on Offshore Mechanics and Arctic Engineering*, vol. 3. New York: ASME; 1988. 379-386.
13. Dodds, R. H., Jr.; Read, D. T. Experimental and numerical studies of the  $J$ -integral for a surface flaw. Submitted to *Int. J. Fract.*
14. Heerens, J.; Read, D. T. Fracture behavior of a pressure vessel steel in the ductile to brittle transition region; NIST 88-3099. Boulder, Colorado: National Institute of Standards and Technology; 1988.
15. Heyliger, P. R.; Kriz, R. D. Calculation of stress intensity factors by enriched mixed finite elements. Submitted to *Commun. Appl. Numer. Methods*.
16. Heyliger, P.; Reddy, J. A higher order beam finite element for bending and vibration problems. Submitted to *J. Sound Vib.*
17. Kim, Y.; Han, J. M.; Lee, J.; Park, C.; Han, J. K.; Reed, R. P. The influence of aluminum and carbon on tensile behavior and microstructure in austenitic Fe-Mn-Al-C alloys. Reed, R. P.; Xing, Z. S.; Collings, E. W., eds. *Cryogenic Materials '88*. Boulder, Colorado: ICMC; 1988. 481-490.
18. Kim, Y.; Lim, C; Ryu, I.; Han, J. K.; Reed, R. P. Low and cryogenic temperature tensile properties of cold-rolled and precipitation hardened copper alloy PMC-102. Reed, R. P.; Xing, Z. S.; Collings, E. W., eds. *Cryogenic Materials '88*. Boulder, Colorado: ICMC; 1988. 693-701.
19. Kriz, R. D.; Ledbetter, H. Graphite-magnesium-composite elastic constants representation surface. Submitted to *Compos. Sci. Technol.*
20. Kohn, G.; Siewert, T. A. Dynamic arc-power source response in GMA welding. Submitted to *Weld. J.*
21. Kriz, R. D.; Sparks, L. L. Performance of alumina/epoxy thermal isolation straps. Clark, A. F.; Reed, R. P., eds. *Advances in Cryogenic Engineering - Materials*, vol. 34. New York: Plenum; 1988. 107-114.
22. Ledbetter, H. M. Elastic properties of metal-oxide superconductors. *J. Met.* 40(1): 24-30; 1988.
23. Ledbetter, H. M.; Austin, M. W. Deformed-polycrystalline-copper elastic constants. *Phys. Status Solidi (a)* 104: 203-212; 1987.
24. Ledbetter, H. M.; Austin, M. W.; Kim, S. A.; Datta, T.; Violet, C. E. Shear-modulus change below  $T_c$  in  $YBa_2Cu_3O_{7-x}$ . *J. Mater. Res.* 2: 790-792; 1987.
25. Ledbetter, H. M.; Austin, M. W.; Kim, S. A.; Lei, M. Elastic constants and Debye temperature of polycrystalline  $Y_1Ba_2Cu_3O_{7-x}$ . *J. Mater. Res.* 2: 786-789; 1987.
26. Ledbetter, H. M.; Kim, S. A. Low-temperature elastic constants of deformed polycrystalline copper. *Mater. Sci. Eng.* 101: 87-92; 1988.

27. Ledbetter, H. M.; Kim, S. A. Molybdenum effect on Fe-Cr-Ni-alloy elastic constants. *J. Mater. Res.* 3: 40-44; 1988.
28. Ledbetter, H. M.; Kim, S. A. Low-temperature manganese contributions to the elastic constants of face-centred-cubic Fe-Cr-Ni stainless steel. *J. Mater. Sci.* 23: 2129-2132; 1988.
29. Ledbetter, H. M.; Kim, S. A.; Austin, M. W.; Datta, T.; Estrada, J.; Violet, C. E. Low-temperature elastic constants of a  $Y_1Ba_2Cu_3O_{7-x}$  superconductor. Submitted to *Phys. Rev. B*.
30. Ledbetter, H. M.; Kim, S. A.; Capone, D. W. Elastic constants of polycrystalline  $Y_1Ba_2Cu_3O_{7-x}$ . *High-Temperature Superconductors II*. Pittsburgh: Mater. Res. Soc.; 1988. 375-378.
31. Ledbetter, H. M.; Kim, S. A.; Datta, T.; Estrada, J.; Violet, C. E. Poisson-ratio anomalies in the  $Y_1Ba_2Cu_3O_{7-x}$  superconductor. Submitted to *Phys. Rev. Lett.*
32. Lin, I.-H. Effect of plate-like rigid inclusions on ductile/brittle transition. Ragunta, R., ed. *Inclusions and Their Influence on Material Behavior*. Metals Park, Ohio: ASM International; 1988. 173-177.
33. Lin, I.-H.; Thomson, R. M. Relativistic BCS-OHR model. *Proceedings, Seventh International Conference on Fracture*. New York: Pergamon. In press.
34. Liu, S.; Siewert, T. A. Metal transfer in gas metal arc welding; droplet frequency. Submitted to *Weld. J.*
35. McCowan, C. N.; Siewert, T. A. Inclusions and fracture toughness in stainless steel welds at 4 K. Clark, A. F.; Reed, R. P., eds. *Advances in Cryogenic Engineering - Materials*, vol. 34. New York: Plenum; 1988. 335-342.
36. McCowan, C. N.; Siewert, T. A.; Kivineva, E. Strength, toughness influence of molybdenum in stainless steel welds for cryogenic service. *Proceedings, AIME Conference on Welding Metallurgy of Structural Steels*. Warrendale, Pennsylvania: Metall. Soc.; 1987. 427-438.
37. McHenry, H. I.; Purtscher, P. T.; Shives, T. R. Observations of hydrogen damage in a failed pressure vessel. *Corrosion Sci.* 27: 1041-1057; 1987.
38. Moulder, J. C.; Nakogawa, N.; Shull, P. T. Progress in uniform field eddy current methods. Thompson, D. O.; Chimenti, D. E. *Review of Progress in Quantitative Nondestructive Evaluation*, vol. 7A. New York: Plenum; 1988. 147-155.
39. Nakajima, H.; Yoshida, K.; Shimamoto, S.; Tobler, R. L.; Purtscher, P. T.; Reed, R. P. Round robin tensile and fracture test results for an Fe-22Mn-13Cr-5Ni austenitic stainless steel at 4 K. Clark, A. F.; Reed, R. P., eds. *Advances in Cryogenic Engineering - Materials*, vol. 34. New York: Plenum; 1988. 241-249.

40. Ogata, T.; Ishikawa, K.; Reed, R. P.; Walsh, R. P. Loading rate effects on discontinuous deformation in load-control tensile tests. Clark, A. F.; Reed, R. P., eds. *Advances in Cryogenic Engineering - Materials*, vol. 34. New York: Plenum; 1988. 233-240.
41. Ogata, T.; Ishikawa, K.; Yuri, T.; Tobler, R. L.; Purtscher, P. T.; Reed, R. P.; Shoji, T.; Nakano, K.; Takahashi, H. Effects of specimen size, side-grooving, and precracking temperature on *J*-integral test results. Clark, A. F.; Reed, R. P., eds. *Advances in Cryogenic Engineering - Materials*, vol. 34. New York: Plenum; 1988. 259-266.
42. Purtscher, P. T.; Reed, R. P. Influence of interstitial content on fracture toughness. Submitted to Proceedings of the International Conference on High Nitrogen Steels. London: Inst. Met. In press.
43. Purtscher, P. T.; Reed, R. P.; Matlock, D. K. Metallographic study of the crack-tip region from fracture mechanics specimens of austenitic and ferritic steels. Submitted to Proceedings of the Materials Research Society Conference. Pittsburgh: Mater. Res. Soc.
44. Purtscher, P. T.; Walsh, R. P.; Reed, R. P. Fracture behavior of 316LN tensile specimen in uniaxial tension at cryogenic temperatures. Clark, A. F.; Reed, R. P., eds. *Advances in Cryogenic Engineering - Materials*, vol. 34. New York: Plenum; 1988. 379-386.
45. Purtscher, P. T.; Walsh, R. P.; Reed, R. P. Design of 316LN-type alloys. Clark, A. F.; Reed, R. P., eds. *Advances in Cryogenic Engineering - Materials*, vol. 34. New York: Plenum; 1988. 165-172.
46. Read, D. T. *J*-integral values for small cracks in steel panels. Read, D. T.; Reed, R. P., eds. *Fracture Mechanics: Eighteenth Symposium*. ASTM STP 945. Philadelphia: Amer. Soc. Test. Mater.; 1988. 151-163.
47. Read, D. T.; Reed, R. P., eds. *Fracture Mechanics: Eighteenth Symposium*. ASTM STP 945. Philadelphia: Amer. Soc. Test. Mater.; 1988. 1117 pp.
48. Reed, R. P. Austenitic stainless steels, with emphasis on strength at low temperatures. Walter, J. L.; Jackson, M. R.; Sims, C. T., eds. *Alloying*. Metals Park, Ohio: ASM International; 1988. 225-256.
49. Reed, R. P., ed. *Materials Studies for Magnetic Fusion Energy Applications at Low Temperatures - XI*. NBSIR 88-3082. Nat. Bur. Stand. (U.S.); 1988. 398 pp.
50. Reed, R. P.; Xing, Z. S.; Collings, E. W., eds. *Cryogenic Materials '88*. Boulder, Colorado: ICMC; 1988. 935 pp.
51. Reed, R. P.; McCowan, C. N.; Walsh, R. P.; Delgado, L. A.; McColskey, J. D. Tensile strength and ductility of indium. *Mater. Sci. Eng. A* 102: 227-236; 1988.
52. Reed, R. P.; Purtscher, P. T.; Delgado, L. A. Low-temperature properties of high-manganese austenitic steels. *High-Manganese Austenitic Steels*. Lula, R. A., ed. Metals Park, Ohio: ASM International; 1988. 13-22.

53. Reed, R. P.; Simon, N. J. Discontinuous yielding in austenitic steels at low temperatures. Reed, R. P.; Xing, Z. S.; Collings, E. W., eds. *Cryogenic Materials '88*. Boulder, Colorado: ICMC; 1988. 851-863.
54. Reed, R. P.; Simon, N. J. Nitrogen strengthening of austenitic stainless steels at low temperatures. Proceedings, International Conference on High Nitrogen Steels. London: Inst. Met. In press.
55. Reed, R. P.; Walsh, R. P. Tensile strain-rate effects in liquid helium. Clark, A. F.; Reed, R. P., eds. *Advances in Cryogenic Engineering - Materials*, vol. 34. New York: Plenum; 1988. 199-208.
56. Reed, R. P.; Walsh, R. P.; Fickett, F. R. Effects of grain size and cold rolling on cryogenic properties of copper. Clark, A. F.; Reed, R. P., eds. *Advances in Cryogenic Engineering - Materials*, vol. 34. New York: Plenum; 1988. 299-308.
57. Reno, R. C.; Fields, R. J.; Clark, A. V. Crystallographic texture in rolled aluminum plates: neutron pole figure measurements. Thompson, D. O.; Chimenti, D. E., eds. *Review of Progress in Quantitative Nondestructive Evaluation*, vol. 7B. New York: Plenum; 1988. 1439-1445.
58. Schramm, R. E.; Clark, A. V., Jr.; Mitracović, D. V.; Shull, P. J. Flaw detection in railroad wheels using Rayleigh-wave EMATs. Thompson, D. O.; Chimenti, D. E. eds. *Review of Progress in Quantitative Nondestructive Evaluation*, vol. 7B. New York: Plenum; 1988. 1661-1668.
59. Schramm, R. E.; Shull, P. J.; Clark, A. V.; Mitraković, D. V. EMAT examination for cracks in railroad wheel treads. Submitted to Proceedings of the Nondestructive Testing and Evaluation for Manufacturing and Construction Conference. Washington, D.C.: Hemisphere Publishing.
60. Schramm, R. E.; Shull, P. J.; Clark, A. V., Jr.; Mitracković, D. V. Emats for roll-by crack inspection of railroad wheels. Submitted to *Review of Progress in Quantitative Nondestructive Evaluation*.
61. Scull, L. L.; Reed, R. P. Tensile and fatigue-creep properties of a copper-stainless steel laminate. Clark, A. F.; Reed, R. P., eds. *Advances in Cryogenic Engineering - Materials*, vol. 34. New York: Plenum; 1988. 397-403.
62. Shimada, M.; Tobler, R. L.; Shoji, T.; Takahashi, H. Specimen size, side-grooving, and precracking effects on *J*-integral test results for SUS 304 stainless steel at 4 K. Clark, A. F.; Reed, R. P., eds. *Advances in Cryogenic Engineering - Materials*, vol. 34. New York: Plenum; 1988. 251-258.
63. Shull, P.; Heyliger, P.; Moulder, J. C.; Gimple, M.; Auld, B. A. Applications of capacitive array sensors to nondestructive evaluation. Thompson, D. O.; Chimenti, D. E. *Review of Progress in Quantitative Nondestructive Evaluation*, vol. 7A. New York: Plenum; 1988. 517-523.
64. Siewert, T. A. Development of a weld procedure to repair joints in precision track. *Weld. J.* 67: 17-23; 1988.

65. Siewert, T. A. Improved standards for real-time radioscopy. Submitted to Proceedings of the ASME Conference and Proceedings of the Department of Defense Conference.
66. Siewert, T. A. Review of 1986 workshop: Computerization of Welding Information. Submitted to Proceedings of the Second Conference and Workshop on Computerization of Welding Information.
67. Siewert, T. A. Standards for real-time radiography—National Bureau of Standards. Submitted to Proceedings, American Society for Nondestructive Testing.
68. Siewert, T. A.; Gorni, D; Kohn, G. High-energy beam welding of type 316LN stainless steel for cryogenic applications. Clark, A. F.; Reed, R. P., eds. *Advances in Cryogenic Engineering - Materials*, vol. 34. New York: Plenum; 1988. 343-350.
69. Siewert, T. A.; Hicho, G. E. Choosing a welding procedure for a ten-meter-long tensile specimen. *Weld. J.* 67: 35-37; 1988.
70. Siewert, T. A.; Jones, J. E.; eds. *Computerization of Welding Information - Report of a Workshop Held August 5-6, 1986 in Knoxville, Tennessee*. Special Publication 742. Nat. Bur. Stand. (U.S.); June 1988. 31 pp.
71. Siewert, T. A.; McCowan, C. N. The role of inclusions in the fracture of austenitic stainless steel welds at 4 K. Koo, J. Y., ed. *Welding Metallurgy of Structural Steels*. Warrendale, Pennsylvania: Metall. Soc.; 1987. 415-425.
72. Siewert, T. A.; McCowan, C. N.; Olson, D. L. Prediction of ferrite number to 100 FN in stainless steel welds. Accepted for publication in vol. 67 of *Weld. J.*
73. Siewert, T. A.; McCowan, C. N.; Vigliotti, D. P. Cryogenic material properties of stainless steel tube-to-flange welds. Submitted to *J. Eng. Mater. Technol.*
74. Simon, N. J.; Reed, R. P. Design of 316LN-type alloys. Clark, A. F.; Reed, R. P., eds. *Advances in Cryogenic Engineering - Materials*, vol. 34. New York: Plenum; 1988. 165-172.
75. Takahashi, H.; Shoji, T.; Tobler, R. L. Acoustic emission and its applications to fracture studies of austenitic stainless steels at 4 K. Clark, A. F.; Reed, R. P., eds. *Advances in Cryogenic Engineering - Materials*, vol. 34. New York: Plenum; 1988. 387-395.
76. Tobler, R. L.; Han, J. K.; Reed, R. P. Fatigue resistance of a 2090-T8E41 aluminum alloy at cryogenic temperatures. Reed, R. P.; Xing, Z. S.; Collings, E. W., eds. *Cryogenic Materials '88*. Boulder, Colorado: ICMC; 1988. 703-712.
77. Tobler, R. L.; Reed, R. P. Proposed standard method for tensile testing of structural alloys at liquid helium temperatures. Reed, R. P., ed. *Materials Studies for Magnetic Fusion Energy Applications at Low Temperatures - XI*. NBSIR 88-3082. Nat. Bur. Stand. (U.S.); 1988. 383-398.

78. Tobler, R. L.; Reed, R. P. Proposed standard method for fracture toughness testing of structural alloys at liquid helium temperatures. Reed, R. P., ed. *Materials Studies for Magnetic Fusion Energy Applications at Low Temperatures - XI*. NBSIR 88-3082. Nat. Bur. Stand. (U.S.); 1988. 363-382.
79. Tobler, R. L.; Trevisan, R. E.; Siewert, T. A.; McHenry, H. I.; Purtscher, P. T.; McCowan, C. N.; Matsumoto, T. Strength, fatigue, and toughness properties of an Fe-18Cr-16Ni-6.5Mn-2.4Mo fully austenitic SMA weld at 4 K. Clark, A. F.; Reed, R. P., eds. *Advances in Cryogenic Engineering - Materials*, vol. 34. New York: Plenum; 1988. 351-358.
80. Violet, C. E.; Datta, T.; Ledbetter, H. M.; Almasen, C.; Estrada, J. Reentrant softening in copper-oxide superconductors. *High-Temperature Superconductors*. Pittsburgh: Mater. Res. Soc.; 1988. 375-378.
81. Yoshida, K.; Nakajima, H.; Oshikiri, M.; Tobler, R. L.; Shimamoto, S.; Miura, R.; Ishizaka, J. Mechanical tests of large specimens at 4 K: facilities and results. Clark, A. F.; Reed, R. P., eds. *Advances in Cryogenic Engineering - Materials*, vol. 34. New York: Plenum; 1988. 225-232.

SELECTED TECHNICAL AND PROFESSIONAL COMMITTEE LEADERSHIP

American Society of Mechanical Engineers  
Boiler and Pressure Vessel Code Committee  
Working Group on Materials, Subgroup on NUPACK, SC III  
S. Yukawa, Chairman  
*Journal of Applied Mechanics*  
R. D. Kriz, Reviewer  
Materials and Structures Group  
S. Yukawa, Immediate Past Vice President

American Society for Testing and Materials  
E07.01: Nondestructive Evaluation  
Task Force on Evaluation of Real-Time Systems  
T. A. Siewert, Member  
E24: Fracture Testing Committee  
E24.06: Fracture Mechanics Applications  
E24.06.05: Fracture Testing of Welds  
H. I. McHenry, Chairman

American Welding Institute  
On-line Welding Data Base Committee  
T. A. Siewert

American Welding Society  
Technical Papers Committee  
T. A. Siewert  
*Welding Journal*  
H. I. McHenry, Reviewer  
T. A. Siewert, Reviewer  
Workshop on Computerization of Welding Data  
Organizing Committee  
T. A. Siewert

ASM International  
Joining Division  
T. A. Siewert, Government Liaison  
*Metallurgical Transactions*  
H. M. Ledbetter, Reviewer

Colorado School of Mines  
R. D. Kriz, Adjunct Professor  
Steel Research Institute Advisory Board  
R. P. Reed

Defense Advanced Research Projects Agency  
Advanced Submarine Technology Program  
Metals Planning Group  
H. I. McHenry

International Cryogenic Materials Conference

Board of Directors

R. P. Reed, Finance Officer

Proceedings

R. P. Reed, Coeditor

International Institute of Welding

Task Group for Elastic-Plastic Fracture-Mechanics Standard

D. T. Read

International Union of Theoretical and Applied Mechanics

Organizing Committee

H. M. Ledbetter

Metals Properties Council

Technical Advisory Committee

R. P. Reed

National Academy of Science

Materials Advisory Group of the Marine Board

T. A. Siewert

NIST-Boulder Editorial Review Board

R. L. Tobler

Superconducting Magnetic-Energy Storage

Technical Advisory Group

R. P. Reed

University of Colorado

Department of Mechanical Engineering Graduate Faculty

R. D. Kriz and H. M. Ledbetter, Adjunct Professors

U.S. Department of Energy, Office of Fusion Energy

Analysis and Evaluation Task Group

N. J. Simon

Joint U.S.-Japanese Exchange Program Advisory Committee

R. P. Reed

Low-Temperature Materials for Magnetic Fusion Energy Committee

R. P. Reed, Coordinator

Magnetics Group, Advisory Committee

R. P. Reed

Versailles Project on Advanced Materials and Standards Task Group

Cryogenic Structural Materials Working Group

R. P. Reed

Welding Research Council

Data Base Task Group

T. A. Siewert

Materials and Welding Procedures Subcommittee

T. A. Siewert

## AWARDS

The Bronze Medal Award for Superior Federal Service was awarded to Alfred V. Clark, Jr. for his leadership and contributions in nondestructive evaluation (NDE) of materials and components. He developed a strong group effort in NDE with emphasis on measurements indicative of structural integrity and reliability, which provide the nation with improved means of assessing the safety of buildings, bridges, and industrial facilities.

At the joint annual meeting of the International Metallographical Society and the American Society for Metals, two division scientists received awards in the International Metallographic Contest. Dominique Shepherd won first prize for her poster, Advantages of Light Microscopy for Measuring Twin Dimensions in High-Temperature Superconductors. Chris McCowan received honorable mention for his contribution, Microstructural Characterization of Y-Ba-Cu-O superconductors.

## INDUSTRIAL AND ACADEMIC INTERACTIONS

### Industrial Interactions

#### Alloy Rods

T. A. Siewert informed researchers at Alloy Rods of the special precautions required for mechanical testing techniques at liquid neon temperature.

#### Amax Materials Research Center

H. M. Ledbetter is studying the elastic constants of pure molybdenum for Amax Materials Research Center in Ann Arbor, Michigan. This material can undergo low-temperature magnetic transitions that may affect the elastic constants of Fe-Cr-Ni-Mo alloys.

#### American Association of Railroads

For the AAR, R. E. Schramm is developing techniques to measure residual stresses and to detect cracks in railroad wheels.

#### American Society for Testing and Materials

T. A. Siewert is coordinating the NIST research on standards for real-time radiography with the relevant ASTM subcommittees. Very close coordination ensures that any image-quality indicators or radiation-transfer standards developed at NIST can be easily transferred to ASTM for consideration as new standards.

#### American Welding Institute and American Welding Society

T. A. Siewert represents NIST on the organizing committee of the 1988 (second) Workshop on Computerization of Welding Data, which is sponsored by NIST, AWI, and AWS. The workshop will review progress over the past two years and develop guidelines for the welding industry in effective use of computers.

#### Battelle Laboratories (Columbus)

H. M. Ledbetter has long-standing collaborations with E. W. Collings on magnetic properties of Fe-Cr-Ni-Mn alloys. Recently they agreed to reopen the studies. They are considering a joint study of the new high- $T_c$  metal-oxide superconductors.

#### CTI Cryogenics

The Welding Group advised CTI Cryogenics on sources of low-temperature properties of solders.

#### Coldren Consulting Company

The Welding Group is working with P. Coldren on a program to develop a new family of high-strength-high-toughness welding consumables. The program will investigate advanced concepts in alloy systems and electrode production techniques.

#### Conoco

A. V. Clark, R. D. Kriz, P. T. Shull, and D. W. Fitting are working with Conoco on the nondestructive evaluation of composites, specifically, monitoring damage with fiber optics. R. E. Schramm provides assistance in the use of EMATs for weld inspection.

#### DuPont

P. T. Shull and A. V. Clark are working with DuPont on the nondestructive evaluation of Kevlar rope.

#### Fax Corporation

R. E. Schramm is working with the Fax Corporation on crack inspection of railroad wheels.

#### Ford Motor Company

A. V. Clark is assisting Ford in the ultrasonic measurement of formability. R. D. Kriz and D. W. Fitting are helping to develop nondestructive evaluation of impact damage in composites.

#### Fusion Technology, Inc.

R. E. Schramm is assisting Fusion Technology in residual-stress measurement in aluminum.

#### Hamilton Standard

T. A. Siewert advised Hamilton Standard on sources for fatigue-crack-growth rates in 2219 base and weld metal.

#### Hercules

P. T. Shull is working with Hercules on the use of eddy-current and capacitive-array probes for nondestructive evaluation of composites.

#### International Institute of Welding

D. T. Read participated in a task group that developed a standard method for reporting fracture-mechanics assessments. The standard will be submitted to the International Standards Organization for consideration as an international standard.

#### McDonnell-Douglas

J. D. McColskey is measuring the mechanical properties of graphite/PEEK composites, which will be used on the national aerospace plane (NASP).

#### Perkin Elmer

H. M. Ledbetter is studying the sound velocities, thermal expansivity, and electrical resistivity of pure beryllium at low temperatures for Perkin Elmer in Danbury, Connecticut. Initial sound-velocity results suggest an unexpected low-temperature transition.

#### Pulano Associates

T. A. Siewert advised Pulano Associates on the use of welding electrodes and the uses of minerals in electrode formulations.

#### Rolled Alloys

T. A. Siewert advised Rolled Alloys on the best mechanical property tests for characterization of stainless steel alloys at 4 K.

#### SCM Metal Products

H. M. Ledbetter is studying the elastic constants of alumina-dispersion-strengthened copper that is manufactured at SCM Metal Products in Cleveland, Ohio. Because the alumina particles are so small (a few hundred angstroms), modeling this material presents an intriguing problem.

#### Toray Industries (Japan)

H. M. Ledbetter, with T. Kyono, is studying the elastic constants of graphite-fiber metal-matrix composites.

#### Union Pacific Railroad

R. E. Schramm is working with the Fax Corporation on crack inspection of railroad wheels.

#### Welding Research Council

T. A. Siewert and J. D. McColskey assist the Materials and Welding Procedures Committee in the development of prequalified welding procedures. The committee is composed of welding fabricators, inspection agencies, insurance companies, sheet-metal workers, and other representatives of the welding industry. It has produced, inspected, tested, and witnessed welds that meet the requirements of fabrication codes. The data from these welds are the basis for new weld-procedure specifications.

## Joint Industrial and Academic Interactions

### Colorado School of Mines

T. A. Siewert is working with H.-G. Lan and S. Liu in the study of droplet transfer in the welding arc. Present emphasis is on development of weld-control techniques that can be implemented by computerized closed-loop systems. The ultimate goal is the development of intelligent controllers for welding processes.

## Academic Interactions

### Colorado School of Mines

The Welding Group, in a joint program with CSM, has analyzed the data from about a thousand stainless steel welds and developed an improved ferrite-prediction diagram for weld metals. The improved accuracy of this diagram will enable the production of welds with more consistent mechanical properties.

A. V. Clark collaborates with D. Matlock on texture and formability research using ultrasonics.

### Davidson College

H. M. Ledbetter collaborates with L. S. Cain of the Physics Department at Davidson College in Davidson, North Carolina in experimental studies of elastic constants. The high-temperature elastic-constant studies of L. S. Cain complement the low-temperature studies of H. M. Ledbetter. Currently, they are studying the carbon-plus-nitrogen alloying effects on Fe-Cr-Ni-alloy elastic constants, which are different at different temperatures.

### Harvard University

The Fracture Physics Group works with H. Gao and J. Rice in studying the three-dimensional image force on a dislocation loops emitted from crack tips.

### Iowa State University: Center for Advanced NDE, Ames Laboratories

A. V. Clark collaborates with R. B. Thompson on texture and formability using ultrasonics.

R. D. Kriz is working with J. C. Moulder, originator of the technique, to improve an optical-strain-measurement system.

### Massachusetts Institute of Technology

The Fracture Physics Group works with A. Argon in studying the brittle-to-ductile transition in cleavage fracture.

#### Osaka University

H. M. Ledbetter began a study with T. Okada on the elastic constants of fiber-reinforced composites.

#### Stanford University

A. V. Clark and P. J. Shull collaborate with B. A. Auld on capacitive array research.

#### Tohoku University

H. M. Ledbetter collaborates with Y. Shindo of the Mechanical Engineering Faculty on problems of waves scattered by interfaces. They use a scattered-plane-wave ensemble-average model.

#### Tsinghua University

H. M. Ledbetter began a study with Y. He: the behavior of low-temperature elastic constants and internal friction of metal-oxide superconductors.

#### University of Arkansas

H. M. Ledbetter, M. W. Austin, and S. A. Kim collaborate with A. M. Hermann of the Physics Department on the physical properties of the new high-critical-temperature metal-oxide superconductors. These properties include electrical resistivity, magnetic susceptibility, elastic constants, and crystal structure (by x-ray diffraction). The studies focus on substituting various trivalent rare-earth cations (R) in the compound  $R_1Ba_2Cu_3O_{7-x}$ .

#### University of Belgrade

D. Mitraković and B. Petrovski were guest workers at NIST in the Nondestructive Evaluation and Fracture Mechanics groups, respectively.

#### University of California

H. M. Ledbetter continues to work with J. Glazer and J. W. Morris, Jr. in studying the low-temperature elastic constants of an Al-Li alloy.

#### University of Cambridge

H. M. Ledbetter works with P. Withers and M. Stobbs of the Metallurgy and Materials Science Department on a theoretical problem of internal stress in composites, stress that arises from differences in the thermal expansivities of the particle and matrix components.

#### University of Colorado

H. M. Ledbetter collaborates with Professor S. Datta on theoretical problems of waves in heterogeneous media. They recently published several joint studies.

#### University of Geneva

Very recently, H. M. Ledbetter began working with B. Seeber to study the elastic constants of Chevrel-phase superconductors.

#### University of Maryland

H. M. Ledbetter collaborates with R. Reno in studies of the effects of texture on elastic constants.

#### University of Michigan

D. W. Fitting is collaborating with researchers at the University of Michigan on the development of silicon-based acoustical arrays.

#### University of South Carolina

H. M. Ledbetter collaborates with T. Datta of the Physics Department on theoretical and experimental studies of low-temperature austenitic-steel physical properties, especially elastic constants and magnetic susceptibility. In these materials, physical properties (and perhaps plastic-deformation properties) depend on the magnetic state. They also study the elastic and magnetic properties of the new high-critical-temperature metal-oxide superconductors, especially  $Y_1Ba_2Cu_3O_{7-x}$ , which shows large elastic and magnetic changes.

H. M. Ledbetter collaborates with R. Edge of the Physics Department on studies of the low-temperature magnetic state in Fe-Cr-Ni alloys. Recently, at Oak Ridge National Laboratory, they obtained new neutron-diffraction results, which they are now trying to interpret.

#### University of Stuttgart

H. M. Ledbetter collaborates with E. Kröner and B. K. D. Gairola on theoretical problems of the elastic constants of polycrystals. They calculated the elastic constants of perfectly random polycrystalline graphite. These new results help to explain the peculiar elastic behavior of two important technological materials: graphite fibers (used in composites) and cast iron.

#### University of Tsukuba

H. M. Ledbetter collaborates with T. Suzuki on both theory and experiment of elastic constants and phase transitions. Currently, they are exchanging ideas on metal-oxide superconductors and on a vibrating-parallelepiped elastic-constant measurement system.

With K. Otsuka, H. M. Ledbetter is studying the elastic constants of the monocystal shape-memory alloy Cu-Al-Ni.

#### University of Washington

H. M. Ledbetter collaborates with M. Taya on problems of elastic constants of and internal strain (residual stress) in composites.

# APPENDIX



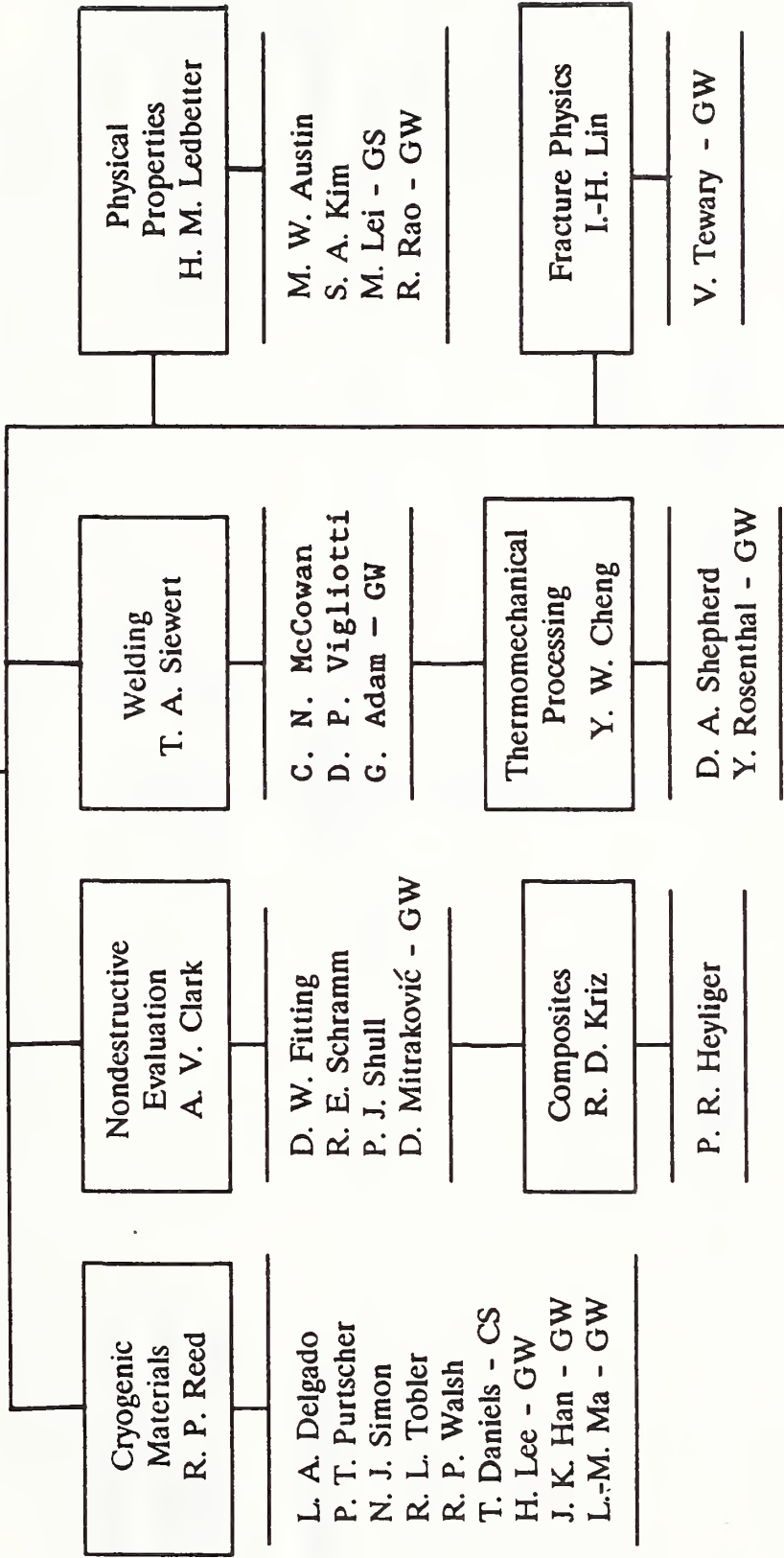
# FRACTURE AND DEFORMATION DIVISION

H. I. McHenry, Chief

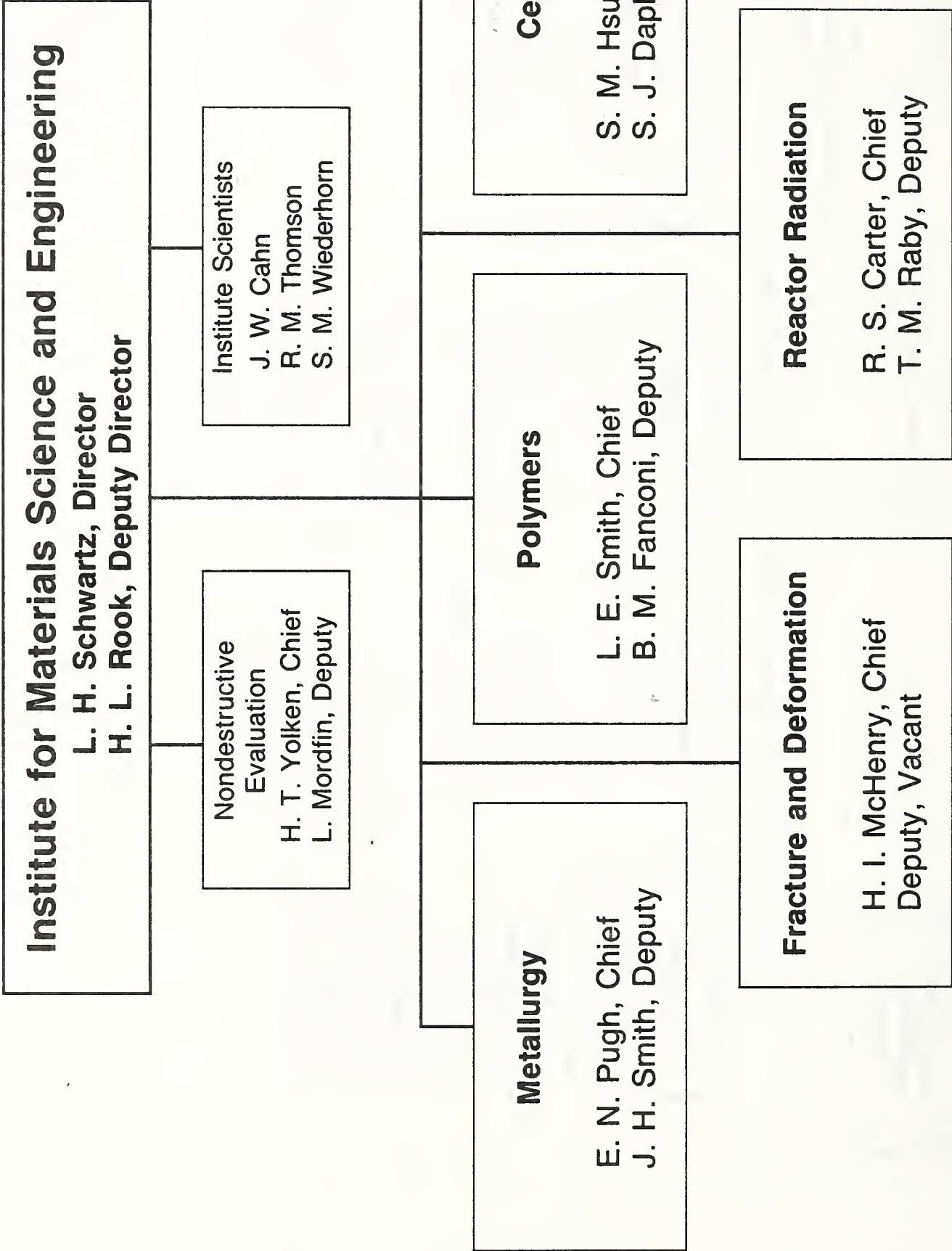
K. S. Sherlock  
Administrative  
Officer

H. M. Quartemont  
Division  
Secretary

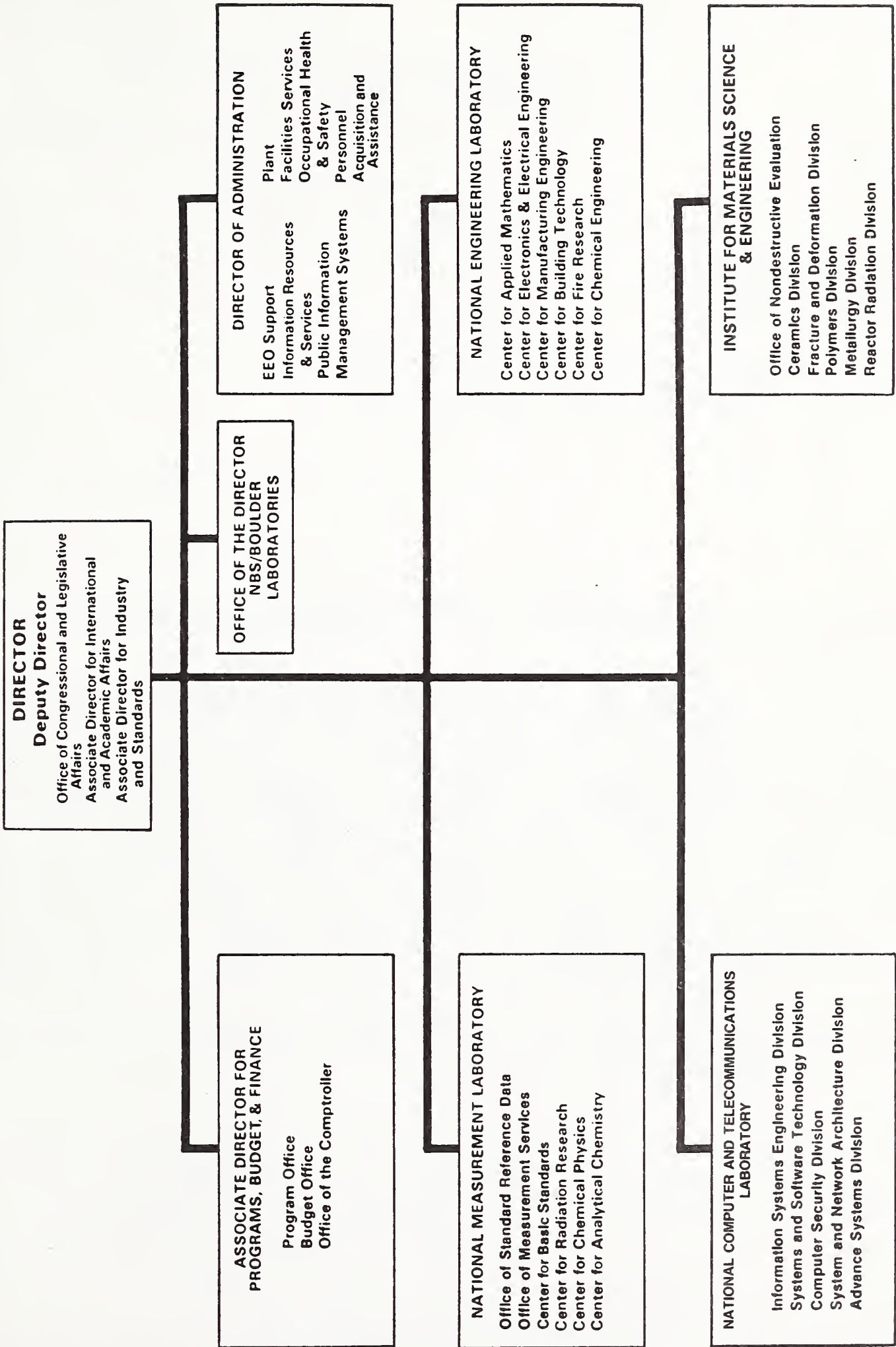
V. J. Edgins, C. J. King, Group Secretaries



CS - Coop student  
GS - Graduate student  
GW - Guest worker



**U.S. DEPARTMENT OF COMMERCE**  
**National Institute of Standards and Technology**



U.S. DEPT. OF COMM. <b>BIBLIOGRAPHIC DATA SHEET</b> <i>(See instructions)</i>	<b>1. PUBLICATION OR REPORT NO.</b> NISTIR 88-3841	<b>2. Performing Organ. Report No.</b>	<b>3. Publication Date</b> FEBRUARY 1989
<b>4. TITLE AND SUBTITLE</b> Institute for Materials Science and Engineering Fracture and Deformation Division Technical Activities 1988			
<b>5. AUTHOR(S)</b>			
<b>6. PERFORMING ORGANIZATION</b> <i>(If joint or other than NBS, see instructions)</i> NATIONAL BUREAU OF STANDARDS DEPARTMENT OF COMMERCE WASHINGTON, D.C. 20234		<b>7. Contract/Grant No.</b>	<b>8. Type of Report &amp; Period Covered</b>
<b>9. SPONSORING ORGANIZATION NAME AND COMPLETE ADDRESS</b> <i>(Street, City, State, ZIP)</i> Fracture and Deformation Division, 430 National Institute of Standards and Technology 325 Broadway Boulder, CO 80303			
<b>10. SUPPLEMENTARY NOTES</b>  <input type="checkbox"/> Document describes a computer program; SF-185, FIPS Software Summary, is attached.			
<b>11. ABSTRACT</b> <i>(A 200-word or less factual summary of most significant information. If document includes a significant bibliography or literature survey, mention it here)</i>  <p>This report describes the 1988 fiscal-year programs of the Fracture and Deformation Division of the Institute for Materials Science and Engineering. It summarizes the principal accomplishments in three general research areas: materials performance, properties, and processing. The Fracture Mechanics, Fracture Physics, Nondestructive Evaluation, and Composite Materials Groups work together to detect damage in metals and composite materials and to assess the significance of the damage with respect to service performance. The Cryogenic Materials and Physical Properties Groups investigate the behavior of materials at low temperature and measure and model the physical properties of advanced materials, including composites, ceramics and the new high-critical-temperature superconductors. The Welding and Thermomechanical Processing Groups investigate the nonequilibrium metallurgical changes that occur during processing and affect the quality, microstructure, properties and performance of metals.</p> <p>The report lists the division's professional staff, their research areas, publications, leadership in professional societies, and collaboration in research programs with industries and universities.</p>			
<b>12. KEY WORDS</b> <i>(Six to twelve entries; alphabetical order; capitalize only proper names; and separate key words by semicolons)</i> composites; cryogenic materials; deformation; fracture; metallurgy; nondestructive evaluation; physical properties; steels; thermomechanical processing; welding			
<b>13. AVAILABILITY</b>  <input checked="" type="checkbox"/> Unlimited <input type="checkbox"/> For Official Distribution. Do Not Release to NTIS <input type="checkbox"/> Order From Superintendent of Documents, U.S. Government Printing Office, Washington, D.C. 20402.  <input checked="" type="checkbox"/> Order From National Technical Information Service (NTIS), Springfield, VA. 22161		<b>14. NO. OF PRINTED PAGES</b>  85	<b>15. Price</b>  \$13.95



